

ผลของระนาบทองคำ(111) ต่อพันธะไฮโดรเจนในคู่เบสของ PNA และ DNA

นายฐิติพงษ์ มีนะโยธิน

วิทยานิพนธ์นี้เป็นส่วนหนึ่งของการศึกษาตามหลักสูตรปริญญาวิทยาศาสตรมหาบัณฑิต
สาขาวิชาเคมี ภาควิชาเคมี
คณะวิทยาศาสตร์ จุฬาลงกรณ์มหาวิทยาลัย
ปีการศึกษา 2556
ลิขสิทธิ์ของจุฬาลงกรณ์มหาวิทยาลัย

บทคัดย่อและแฟ้มข้อมูลฉบับเต็มของวิทยานิพนธ์ตั้งแต่ปีการศึกษา 2554 ที่ให้บริการในคลังปัญญาจุฬาฯ (CUIR)
เป็นแฟ้มข้อมูลของนิสิตเจ้าของวิทยานิพนธ์ที่ส่งผ่านทางบัณฑิตวิทยาลัย

The abstract and full text of theses from the academic year 2011 in Chulalongkorn University Intellectual Repository (CUIR)
are the thesis authors' files submitted through the Graduate School.

EFFECT OF AU(111) ON HYDROGEN BONDS IN PNA AND DNA BASE
PAIRS

Mr. Thitiphong Meenayothin

A Thesis Submitted in Partial Fulfillment of the Requirements
for the Degree of Master of Science Program in Chemistry
Department of Chemistry
Faculty of Science
Chulalongkorn University
Academic Year 2013
Copyright of Chulalongkorn University

Thesis Title EFFECT OF AU(111) ON HYDROGEN BONDS IN PNA
 AND DNA BASE PAIRS
By Mr. Thitiphong Meenayothin
Field of Study Chemistry
Thesis Advisor Assistant Professor Viwat Vchirawongkwin, Dr. rer. nat.

Accepted by the Faculty of Science, Chulalongkorn University in Partial Fulfillment of the Requirements for the Master's Degree

.....Dean of the Faculty of Science
(Professor Supot Hannongbua, Dr. rer. nat.)

THESIS COMMITTEE

.....Chairman
(Professor Tirayut Vilaivan, D.Phil.)

.....Thesis Advisor
(Assistant Professor Viwat Vchirawongkwin, Dr. rer. nat.)

.....Examiner
(Assistant Professor Somsak Pianwanit, Ph.D.)

.....External Examiner
(Associate Professor Chinapong Kritayakornupong, Dr. rer. nat.)

รุติพงษ์ มีนะโยธิน : ผลของระนาบทองคำ(111) ต่อพันธะไฮโดรเจนในคู่เบสของ PNA และ DNA. (EFFECT OF AU(111) ON HYDROGEN BONDS IN PNA AND DNA BASE PAIRS) อ.ที่ปรึกษาวิทยานิพนธ์หลัก : ผศ. ดร.วิวัฒน์ วชิรวงศ์กวิน, 75 หน้า.

การตรวจสอบผลกระทบจากระนาบทองคำที่เกิดขึ้นกับความหนาแน่นอิเล็กตรอนรวมถึงการเปลี่ยนแปลงโครงสร้างคู่เบสของ DNA และ PNA ด้วยข้อมูลจากการคำนวณ โดยใช้ชุดฐานหลัก 6-311++G(d,p) สำหรับคำนวณโครงสร้างของกรดนิวคลีอิก และใช้ชุดฐานหลัก LANL2DZ สำหรับหาคำนวณระนาบทองคำ(111) ที่ระดับ B3LYP เพื่อสร้างฟังก์ชันคลื่นไปใช้ในการวิเคราะห์ด้วยทฤษฎีอะตอมโมเลกุล ผลการศึกษาแสดงให้เห็นว่าพันธะไฮโดรเจนของคู่เบสภายในโครงสร้างของ PNA ได้รับผลกระทบให้มีความแข็งแรงเพิ่มขึ้นมากกว่าพันธะไฮโดรเจนของคู่เบสภายในโครงสร้างของ DNA ยกเว้นพันธะไฮโดรเจนระหว่างอะตอมไนโตรเจนกับไฮโดรเจนของคู่เบสกวีนีนและไซโทซีนในโครงสร้าง DNA โครงสร้างของ PNA มีแนวโน้มของการเปลี่ยนแปลงโครงสร้างเป็นไปในทางเดียวกันทุกโครงสร้าง ในขณะที่โครงสร้างของ DNA มีความแปรผันสูง สำหรับผลกระทบของสนามไฟฟ้าที่เกิดขึ้นกับพันธะไฮโดรเจนภายในโครงสร้างของคู่เบสที่ร่วมกับระนาบทองคำ(111) ผลการศึกษาแสดงให้เห็นถึงแนวโน้มที่เกิดขึ้นมีสี่ประเภท ได้แก่ การเปลี่ยนแปลงที่ขึ้นกับขนาดและทิศทางของสนามไฟฟ้า การเปลี่ยนแปลงที่ขึ้นกับขนาดของสนามไฟฟ้าในทิศทางเดียว การเปลี่ยนแปลงที่ขึ้นกับขนาดแต่ไม่ขึ้นกับทิศทางของสนามไฟฟ้า และการเปลี่ยนแปลงที่ไม่สามารถบ่งบอกแนวโน้มได้

ภาควิชา.....เคมี..... ลายมือชื่อนิสิต.....
 สาขาวิชา.....เคมี..... ลายมือชื่อ อ.ที่ปรึกษาวิทยานิพนธ์หลัก.....
 ปีการศึกษา.....2556.....

5471958723 : MAJOR CHEMISTRY

KEYWORDS : AIM/H-Bond/DNA/PNA

THITIPOHNG MEENAYOTHIN : EFFECT OF AU(111) ON HYDROGEN BONDS IN PNA AND DNA BASE PAIRS. ADVISOR : ASST. PROF. VI-WAT VCHIRAWONGKWIN, Dr. rer. nat., 75 pp.

The structures of DNA and peptide nucleic acid (PNA) base pairs were affected in the electron density toward the geometry change by Au(111), which were investigated using the 6-311++G(d,p) basis set for nucleic acid structures and LANL2DZ basis set for Au(111) at B3LYP level to generate the wave functions for analysis in the atoms in molecules theory (AIM). The results indicated that the hydrogen bond interactions within the PNA structures experience stronger effects than DNA except N...H of guanine and cytosine (GC) base pairs. PNA has the same tendency of the structure change in every conformer while DNA has a high variability. For the effect of electric field on base pair structures combined with Au(111), the results manifest four categories of the tendency: depending on the electric field intensity and direction, depending on the intensity of electric field in one direction, depending on the electric field intensity but independent of the electric field direction, and a trend that cannot be classified.

Department :Chemistry..... Student's Signature.....

Field of Study :Chemistry..... Advisor's Signature.....

Academic Year :2013.....

ACKNOWLEDGEMENTS

This thesis was successfully finished with the tremendous support from my advisor, Assist. Prof. Dr.Viwat Vchirawongkwin. I would especially like to thank you for his guidance, praiseworthy attitude and friendship. His mentorship was crucial in bestowing a well rounded experience for my future goal.

I would also like to specially thank Prof. Dr.Tirayut Vilaivan, Assoc. Prof. Dr.Chinapong Kritayakornupong and Assist. Prof. Dr.Somsak Pianwanit who acted as the thesis exam committee members and took the time to inspect and comment on this thesis.

Furthermore, I would like to thank Prof. Dr.Supot Hannongbua and the Department of Chemistry, Faculty of Science, Chulalongkorn University for the support of the infrastructure for the calculations.

Finally, I would like to acknowledge my family and friends for their belief in me and embolden me to strive towards my goal.

CONTENTS

	Page
ABSTRACT IN THAI	iv
ABSTRACT IN ENGLISH	v
ACKNOWLEDGEMENTS	vi
CONTENTS	vii
LIST OF TABLES	ix
LIST OF FIGURES	x
CHAPTER I INTRODUCTION	1
CHAPTER II METHODS	4
2.1 Computer Simulation	4
2.1.1 Molecular Dynamics	4
2.2 Density Functional Theory	5
2.3 Atoms in Molecules	7
2.3.1 Topological properties of the charge density	8
2.3.2 Bond paths and Molecular graphs	10
2.3.3 Bond properties	10
CHAPTER III COMPUTATIONAL DETAILS	12
3.1 Geometry relaxations of DNA and PNA structures	12
3.2 Geometry profiles of model structures	12
CHAPTER IV RESULTS AND DISCUSSIONS	17
4.1 Investigations of the effect of Au(111)	18
4.1.1 Topological properties of interaction analysis	18
4.1.2 Topological properties of geometrical analysis	20
4.2 Investigations of the electric field effect on complex structures	27
4.2.1 Topological properties of interaction analysis	27

	Page
4.2.2 Topological properties of geometrical analysis	34
4.2.3 Electronic properties investigation on complex structures . . .	38
CHAPTER V CONCLUSION	40
REFERENCES	47
APPENDIX	48
VITAE	75

LIST OF TABLES

Table	Page
4.1 Bond path length (a.u.) of the $(3, -1)$ bond critical point (BCP) to each nuclei associated with the hydrogen bonds between adenine (A) and thymine (T) base pairs	21
4.2 Bond path length (a.u.) of the $(3, -1)$ bond critical point (BCP) to each nuclei associated with the hydrogen bonds between guanine (G) and cytosine (C) base pairs	22
A1 Topological properties of the electron density at the $(3, -1)$ bond critical point (BCP) of the hydrogen bond interactions between adenine (A) and thymine (T) base pairs	49
A2 Topological properties of the electron density at the $(3, -1)$ bond critical point (BCP) of the hydrogen bond interactions between guanine (G) and cytosine (C) base pairs	51
A3 Topological properties of the electron density at the $(3, -1)$ bond critical point (BCP) of the hydrogen bond interactions between adenine (A) and thymine (T) base pairs	53
A4 Topological properties of the electron density at the $(3, -1)$ bond critical point (BCP) of the hydrogen bond interactions between guanine (G) and cytosine (C) base pairs	59
A5 Bond path length (a.u.) of the $(3, -1)$ bond critical point (BCP) to each nuclei associated with the hydrogen bonds between adenine (A) and thymine (T) base pairs	68
A6 Bond path length (a.u.) of the $(3, -1)$ bond critical point (BCP) to each nuclei associated with the hydrogen bonds between guanine (G) and cytosine (C) base pairs	71
A7 Energy gap profiles of the base pair structures combined with Au(111) were applied in the electric field.	74

LIST OF FIGURES

Figure	Page
1.1 The model structure of DNA and PNA.	2
3.1 The structure of DNA and PNA.	13
3.2 The graph shows the MD simulations results of DNA and PNA structures; (a) resulted graph of (AT) base pairs within DNA structure, (b) resulted graph of (GC) base pairs within DNA structure and (c) resulted graph of PNA structure	14
3.3 Model structures of the base pairs were stacked by Au(111).	16
3.4 Detailed structure in the side view.	16
4.1 The definition of the positions of hydrogen bond interactions in base pairs.	17
4.2 The ellipticity change of the hydrogen bond interactions between adenine (A) and thymine (T) base pairs.	19
4.3 The ellipticity change of the hydrogen bond interactions between guanine (G) and cytosine (C) base pairs.	20
4.4 The representative of the molecular orbitals of the isolated structure and the structure combined with Au(111) that involved with the hydrogen bonds.	24
4.5 The density of state profiles of (a) the isolated structure and (b) the structure combined with Au(111).	25
4.6 The molecular orbitals energy profiles of the isolated structure and the structure combined with Au(111) that involved with the hydrogen bonds.	26
4.7 The tendency of ellipticity change of the hydrogen bond interactions between adenine (A) and thymine (T) base pairs.	29
4.8 The tendency of ellipticity change of the hydrogen bond interactions between guanine (G) and cytosine (C) base pairs.	32

4.9	The tendency of bond path change of the hydrogen bond interactions between adenine (A) and thymine (T) base pairs.	35
4.10	The tendency of bond path change of the hydrogen bond interactions between guanine (G) and cytosine (C) base pairs.	37
4.11	Energy gap profiles of the base pair structures combined with Au(111) were applied in the electric field.	39

CHAPTER I

INTRODUCTION

DNA is a major component of various kinds in biological organisms, which help determine their characteristics by using the genetic code of the base sequence. At present, DNA can be modified into PNA by changing the structure of the backbone [1] (Figure 1.1) to develop therapeutic agents, diagnostics and medicinal applications [2–11]. The results of many researches of PNA have shown a high nucleic acid binding affinity, and high chemical and biological stability [12–15]. Moreover, both patterns and properties of DNA and PNA structures are interesting. For instance, both of them used base sequences for coding and also used hydrogen bond interactions to match the base pairs, indicating that the bases and chemical interactions have a significant role to control the characteristics of their structure. From the aforementioned concepts, they can be applied to be molecular devices in further researches from the fundamental knowledge of chemical interactions.

Hydrogen bond interactions are important in biological processes and fundamental knowledge to understanding the chemical properties [16–18]. They are also a main factor to stabilize the DNA double helix [19,20]. Therefore, the change of hydrogen bonds affects on the alteration in DNA and PNA structures such as the denaturation by heat or chemical substances, and the protein biosynthesis process: the DNA structure in replication, transcription and translation processes that vary due to a modification in hydrogen bonds in various conditions of enzymes [21,22]. Heretofore, the properties and the effects on DNA structure, PNA structure and hydrogen bond interactions between the base pairs are described by many publications. Natsume et al. [23] considered the electronic properties of hybridized DNA-DNA, PNA-DNA and PNA-PNA double strands by density functional theory (DFT) calculations, suggesting that the strength of the hybridization be sorted by descending

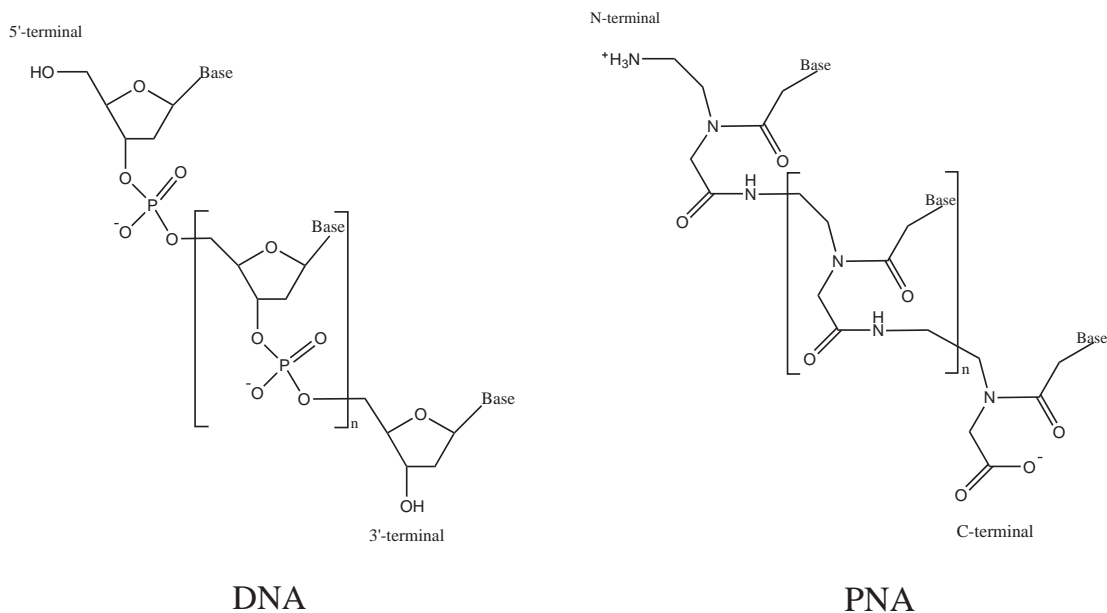


Figure 1.1: The model structure of DNA and PNA.

like PNA-PNA, PNA-DNA and DNA-DNA double strands, respectively. On the other hand, Lv et al. [24] proposed that the small gold clusters have a significant role in the complexation process with thymine base by DFT calculations. Withal, Valdespino-Saenz and Martinez [25] contemplated non-conventional hydrogen bonds in the neutral molecules of adenine-Au and adenine-uracil-Au utilizing DFT calculations. Their results displayed the non-conventional hydrogen bonds rarely occur when compared to the structures of cation and anion. Recently, Maeda et al. [26] investigated the hydration effect on the electrical conductivity of DNA structures, indicating that the solvated DNA duplexes have more electrical conductivity than its gas phase using Au electrodes via the analysis of Green's function combined with DFT.

In order to investigate hydrogen bonds in an electronic structure, the calculations require a high theoretical level to obtain the high accuracy results. Nevertheless, both DNA and PNA structures are large and complicated molecules. It is difficult to optimize their structures for consideration of the change of electronic structures and properties. Thus, we proposed an alternative method to solve these problems by the investigation of electronic structural change without altering the molecular structure by single point calculations of isolated structure and complex structure to generate

the different wave functions in order to compare and contemplate the differences. Moreover, we also consider the effect on hydrogen bonds within an electric field by applying point charges on each structure.

To analyze the wave functions, the atoms in molecules theory (AIM) is one of methods that can explain the properties of hydrogen bond interactions [16,27]. This method employs the topologies in terms of an electron density distribution function to analyze the chemical bond strength, which can be prosperously used to discriminate weak, medium, and strong hydrogen bonds in different molecular systems [16,20,28]. In this work, we investigated the structures of DNA and PNA affected on the electron density toward the geometry change by Au(111), in which we considered the hydrogen bonds between base pairs by performing AIM analysis, in order to obtain some properties of the electron density to demonstrate the change in their behaviors.

CHAPTER II

METHODS

2.1 Computer Simulation

The calculations of the molecular properties usually utilize the ab initio and density functional theory methods. These have limitations relatively demanding of computer resources. Therefore, the evaluation can be done with molecular systems that are small and less complicated at absolute zero temperature. In most experiments on chemical properties, the molecular systems are in a solution at room temperature and rather complicated structure. The effective in the calculations by the aforementioned methods is unsuitable to predict and understand the ‘real’ world properties. Simulation methods have been developed to investigate such systems base on statistical mechanics yielding micro- and macroscopic quantities, which can be compared with experimental data. Metropolis and coworkers presented the Metropolis Monte Carlo (MC) method, which is the first computer simulation of a molecular system [29]. Theirs aims to generate a history of configurations from a chosen statistical ensemble, which are not connected in time. The second method is Molecular Dynamics (MD), which was developed to investigate the dynamics of a system based on Newtonian mechanics [30,31]. The MD simulation has been examined on the molecular systems of this thesis.

2.1.1 Molecular Dynamics

The classical MD simulations require the construction of the two-body and three-body potentials, generating the system configurations based on Newton’s laws of motion. In the case of the force (\vec{F}) exerted on the particle, the particle with mass (m) moves with an acceleration ($\vec{a} = \frac{d^2\vec{r}}{dt^2}$) in accordance with Newton’s second

laws,

$$\vec{F} = m \frac{d^2 \vec{r}}{dt^2}. \quad (2.1)$$

The force can be manifested as the gradient of the potential energy (\mathcal{V}),

$$\vec{F} = -\nabla \mathcal{V}. \quad (2.2)$$

By coalescing eq. (2.1) and eq. (2.2), a trajectory can be generated which specifies the positions and velocities of particles in the system as a function of time. Nevertheless, the total potential energy for the N -particle system is very complicated owing to the influence of many-body interactions,

$$\mathcal{V}_{total} = \sum_i \mathcal{V}_1(i) + \sum_{j>i} \mathcal{V}_2(i, j) + \sum_{k>j>i} \mathcal{V}_3(i, j, k) + \dots + \sum_{N>\dots>k>j>i} \mathcal{V}_N(i, j, k, \dots, N). \quad (2.3)$$

2.2 Density Functional Theory

The foundation of density functional theory based on a mathematical theorem that the total energy of the ground state for a many electron system is expressed by a universal functional of electron density, $\rho(r)$. The related theorems were stated by Hohenberg, Kohn and Sham [32, 33]. A functional is a function of a “definite” to transform a density function into the electronic energy. Hohenberg and Kohn expressed the first theorem that the total energy (E) of the non-degenerate ground state for a many electron system uniquely determined by a functional of electron density, $\rho(r)$. The total energy of the ground state is given by a universal functional of the electron density as:

$$E[\rho] = \int \rho(r) v(r) dr + F[\rho(r)], \quad (2.4)$$

where $F[\rho(r)]$ is the sum of the kinetic energy and electron-electron interactions. According to the first theorem and the variational principle, it is found that

$$\langle \tilde{\Psi} | H | \tilde{\Psi} \rangle = \int \tilde{\rho}(r) v(r) + F[\tilde{\rho}] > E[\rho], \quad (2.5)$$

where $\tilde{\Psi}$ is not the true wave function of H . Therefore, the second theorem was expressed by Hohenberg and Kohn, which is the total energy ($E[\rho]$) of the ground state, obtained by minimizing the total energy functional with respect to the electron density. That is,

$$E[\rho] = \min_{\rho} E[\rho]. \quad (2.6)$$

For the third theorem, the $\rho(r)$ of the ground state is uniquely determined by a single particle external potential, $v(r)$. Then, Kohn and Sham expressed the fourth theorem that the total energy of the ground state for a many electron system is determined by solving self-consistently the equation with an effective single particle potential, v_{eff} , calculated by the $\rho(r)$. The Kohn-Sham expression for the electronic energy functional is given by:

$$E[\rho(r)] = T_s + E_{en} + E_{ee} + E_{xc} \quad (2.7)$$

$$T_s = \sum_i n_i \int \psi_i(r) \left(-\frac{1}{2} \nabla^2 \right) \psi_i(r) dr \quad (2.8)$$

$$E_{en} = - \sum_{\alpha} \int \frac{Z_{\alpha} \rho(r)}{|r - R_{\alpha}|} dr \quad (2.9)$$

$$E_{ee} = \frac{1}{2} \iint \frac{\rho(r_1) \rho(r_2)}{|r_1 - r_2|} dr_1 dr_2 \quad (2.10)$$

$$\left(-\frac{1}{2} \nabla^2 + v_{eff}(r) \right) \psi_i(x) = \epsilon_i \psi_i(x) \quad (2.11)$$

$$v(r) = - \sum_{\alpha} \frac{Z_{\alpha}}{|r - R_{\alpha}|} + \int \frac{\rho(r')}{|r - r'|} dr' + \frac{\delta E_{xc}[\rho]}{\delta \rho(r)} \quad (2.12)$$

$$\rho_{eff}(r) = 2 \sum_i n_i |\psi_i(r)|^2 \quad (2.13)$$

$$n_i = \theta(\mu - \epsilon_i) \equiv \begin{cases} 1 & (\epsilon_i < \epsilon_F) \\ 0 & (\epsilon_i > \epsilon_F) \end{cases} \quad (2.14)$$

where T_s is the non-interacting kinetic energy, E_{en} describes the electron-nuclei interaction, E_{ee} is the classical electrostatic repulsion energy among the electrons, and E_{xc} is the exchange-correlation energy functional, correcting the electron-electron repulsion. The fifth theorem states in Janak's theorem [34] that a single particle energy, ϵ_i , of the Kohn-Sham orbital relates to the variation of the total energy with respect to an occupation number n_i as:

$$\epsilon_i = \frac{\partial E[\rho]}{\partial n_i}. \quad (2.15)$$

A hybrid exchange-correlation functional is a linear combination of the Hartree-Fock exact exchange functional (E_X^{HF}) and an exchange and correlation density functionals. The popular hybrid functional, namely the Becke three-parameter exchange functional and the dynamic correlation functional of Lee, Yang and Parr (B3LYP) [35–38], is defined as eq. (2.16). The a , b and c parameters are the prediction and the experimental data fitting, and depend on the forms of E_x^{GGA} and E_c^{GGA} . E_x^{LSDA} , E_x^{exact} and E_x^{B88} are exchange functional terms, while E_c^{LSDA} and E_c^{LYP} are the correlation functional terms.

$$E_{XC}^{B3LYP} = (1 - a)E_x^{LSDA} + aE_x^{exact} + b\Delta E_x^{B88} + (1 - c)E_c^{LSDA} + cE_c^{LYP}. \quad (2.16)$$

It was found that $a = 0.20$, $b = 0.72$ and $c = 0.8$.

2.3 Atoms in Molecules

The fundamental idea for the quantum theory of atoms in molecules (QTAIM) is that molecular properties can be determined from quantum observables such as the electron density, $\rho(\mathbf{r})$, and energy densities, developed by Richard F.W. Bader and his coworkers [28]. This theory defines that atoms are objects in real space as determined by the topological properties of a molecular charge distribution.

2.3.1 Topological properties of the charge density

The topology of the electron density is dominated by the attractive forces of the nuclei. In general, the positions of the nuclei manifest the local maxima of charge density (ρ). These consequence are determined by the balance in the forces of the neighboring nuclei exert on the electrons. In topological features of $\rho(\mathbf{r})$, a maximum, a minimum, or saddle point in space is a “critical point” whereat the first derivatives of the density vanish,

$$\nabla\rho = \mathbf{i}\frac{d\rho}{dx} + \mathbf{j}\frac{d\rho}{dy} + \mathbf{k}\frac{d\rho}{dz} \begin{cases} = \vec{0} & \text{(At critical points and at } \infty) \\ \text{Generally } \neq \vec{0} & \text{(At all other points)} \end{cases} \quad (2.17)$$

where the zero vector signifies that derivatives in the gradient operator (∇) is zero. The second derivatives can discriminate a local minimum, a local maximum, or a saddle point. There are nine second derivatives of $\rho(\mathbf{r})$ called the “Hessian matrix”. Their evaluated at the position of the critical point \mathbf{r}_c is given by

$$\mathbf{A}(\mathbf{r}_c) = \begin{pmatrix} \frac{\partial^2\rho}{\partial x^2} & \frac{\partial^2\rho}{\partial x\partial y} & \frac{\partial^2\rho}{\partial x\partial z} \\ \frac{\partial^2\rho}{\partial y\partial x} & \frac{\partial^2\rho}{\partial y^2} & \frac{\partial^2\rho}{\partial y\partial z} \\ \frac{\partial^2\rho}{\partial z\partial x} & \frac{\partial^2\rho}{\partial z\partial y} & \frac{\partial^2\rho}{\partial z^2} \end{pmatrix}_{\mathbf{r}=\mathbf{r}_c}. \quad (2.18)$$

This matrix is real and symmetric which can be diagonalized. The diagonalization of $\mathbf{A}(\mathbf{r}_c)$ corresponds to a rotation of the $\mathbf{r}(x, y, z)$ coordinate system superimposing the new axes $\mathbf{r}'(x', y', z')$ coordinate with the principal of the critical point. The diagonalized form of \mathbf{A} (Λ) is written as:

$$\Lambda = \begin{pmatrix} \frac{\partial^2\rho}{\partial x'^2} & 0 & 0 \\ 0 & \frac{\partial^2\rho}{\partial y'^2} & 0 \\ 0 & 0 & \frac{\partial^2\rho}{\partial z'^2} \end{pmatrix}_{\mathbf{r}'=\mathbf{r}_c} = \begin{pmatrix} \lambda_1 & 0 & 0 \\ 0 & \lambda_2 & 0 \\ 0 & 0 & \lambda_3 \end{pmatrix}, \quad (2.19)$$

where λ_1, λ_2 , and λ_3 are the curvature of the density with respect to the three principal axes x', y', z' . The summation of their diagonal elements is invariant to the rotations of the coordinate system. Therefore, the trace of the Hessian matrix of the density, when $x = x', y = y'$ and $z = z'$, is known as the Laplacian of the density ($\nabla^2\rho(r)$),

$$\nabla^2\rho(r) = \nabla \cdot \nabla\rho(r) = \underbrace{\frac{\partial^2\rho(r)}{\partial x^2}}_{\lambda_1} + \underbrace{\frac{\partial^2\rho(r)}{\partial y^2}}_{\lambda_2} + \underbrace{\frac{\partial^2\rho(r)}{\partial z^2}}_{\lambda_3}. \quad (2.20)$$

The critical points can be classified by rank (ω) and signature (σ) labeled by (ω, σ) . The rank is the number of non-zero eigenvalues for the density at the critical point. The signature is the algebraic sum of the signs for the eigenvalues. In general, the critical points of charge distributions for molecules that stable in geometrical configurations of the nuclei are rank three ($\omega = 3$). Thus, there are four types of critical points in rank three:

- (3, -3) Three negative eigenvalues: ρ is a local maximum.
- (3, -1) Two negative eigenvalues: ρ is a maximum in the plane defined by the corresponding eigenvectors and a minimum along the third axis which is perpendicular to this plane.
- (3, +1) Two positive eigenvalues: ρ is a minimum in the plane defined by the corresponding eigenvectors and a maximum along the third axis which is perpendicular to this plane.
- (3, +3) Three positive eigenvalues: ρ is a local minimum.

From the aforementioned types of critical points, these are identified with an element of chemical structure: (3, -3) nuclear critical point (NCP); (3, -1) bond critical point (BCP); (3, +1) ring critical point (RCP); and (3, +3) cage critical point (CCP).

2.3.2 Bond paths and Molecular graphs

The “bond path” is a line of two gradient paths originating at the bond critical point, and terminates at the neighbouring attractors. This line is a single line of local maximum density, linking the nuclei through the charge distribution. The point on the bond path with the lowest value of the electron density is the bond critical point, separating the two bonded atoms at a zero-flux surface of bond path intersection. The molecular graph is the collection of bond paths linking the nuclei of bonded atoms in the equilibrium geometry.

2.3.3 Bond properties

A zero-flux surface is defined by a set of $\nabla\rho(r)$ trajectories terminating at the bond critical point ($\nabla\rho(r) = 0$). The value of the electron density at a bond critical point determines the strength of a chemical bond, namely bond order (BO):

$$\text{BO} = \exp[A(\rho_b - B)], \quad (2.21)$$

where A and B are constants depending on the nature of the bonded atoms. In general, the electron density at the bond critical point is greater than 0.2 a.u. in shared interaction and less than 0.1 a.u. in closed-shell interaction. For the Laplacian of the electron density at the bond critical point ($\nabla^2\rho_b$), there is the sum of three eigenvalues of the density at a bond critical point. Its two eigenvalues (λ_1, λ_2) are perpendicular to the bond path, which are negative. On the contrary, the third eigenvalue (λ_3) lying along the bond path is positive. The density of negative eigenvalues is concentrated along the bond path while the density of positive eigenvalue is depleted in the region of the inter-atomic surface and concentrated in the individual atomic basins. The two negative eigenvalues are dominant and $\nabla^2\rho_b < 0$ within shared interaction, whereas the positive eigenvalue is prominent and $\nabla^2\rho_b > 0$ within closed-shell interaction. Ultimately, the bond ellipticity (ε) provides a measure of the extent to which electron density is preferentially accumulated in a given plane. The ellipticity is defined as:

$$\varepsilon = \frac{\lambda_1}{\lambda_2} - 1 \quad (\text{where } |\lambda_1| \geq |\lambda_2|). \quad (2.22)$$

If λ_1 equals λ_2 , the ε is zero, the bond is cylindrically symmetrical.

CHAPTER III

COMPUTATIONAL DETAILS

3.1 Geometry relaxations of DNA and PNA structures

Both DNA structures of Adenine-Thymine (AT) and Guanine-Cytosine (GC) having ten base pairs were constructed by Nucgen in AMBER9 [39] program. PNA structure was downloaded from Protein Data Bank (PDB) with 1PUP code. Their structures are shown in Figure 3.1.

In order to neutralize the negative charges of DNA structures, the counter ions (Na^+) were added to each PO_4^{3-} moiety of DNA backbones. The structure of DNA and PNA were relaxed by the classical molecular dynamic (MD) simulations via AMBER9 program, because the nucleic acid structure is very flexible that can be easily affected by a thermal fluctuation and solvents in the environment [26,40,41]. The TIP3P [42] force fields were employed to configure the water molecules that solvate around DNA and PNA structures within 10 Angstroms. The MD simulations were performed in the canonical ensemble (NVT) at 300K with a total simulation time of 1 nanosecond and a time-step of 1 femtosecond. The equilibrated structures and the MD simulations results are shown in Figure 3.2.

3.2 Geometry profiles of model structures

We extracted the central base pair fragments with the backbone residues from each simulated structure that have the lowest energy. The asymmetric ends at the backbone were terminated by hydrogen atoms. Then, we attached Au(111) to their structure as shown in Figure 3.3 and Figure 3.4. The Au(111) model is comprised of six triangularly-planar Au atoms, which were stacked up along with one base. One edge

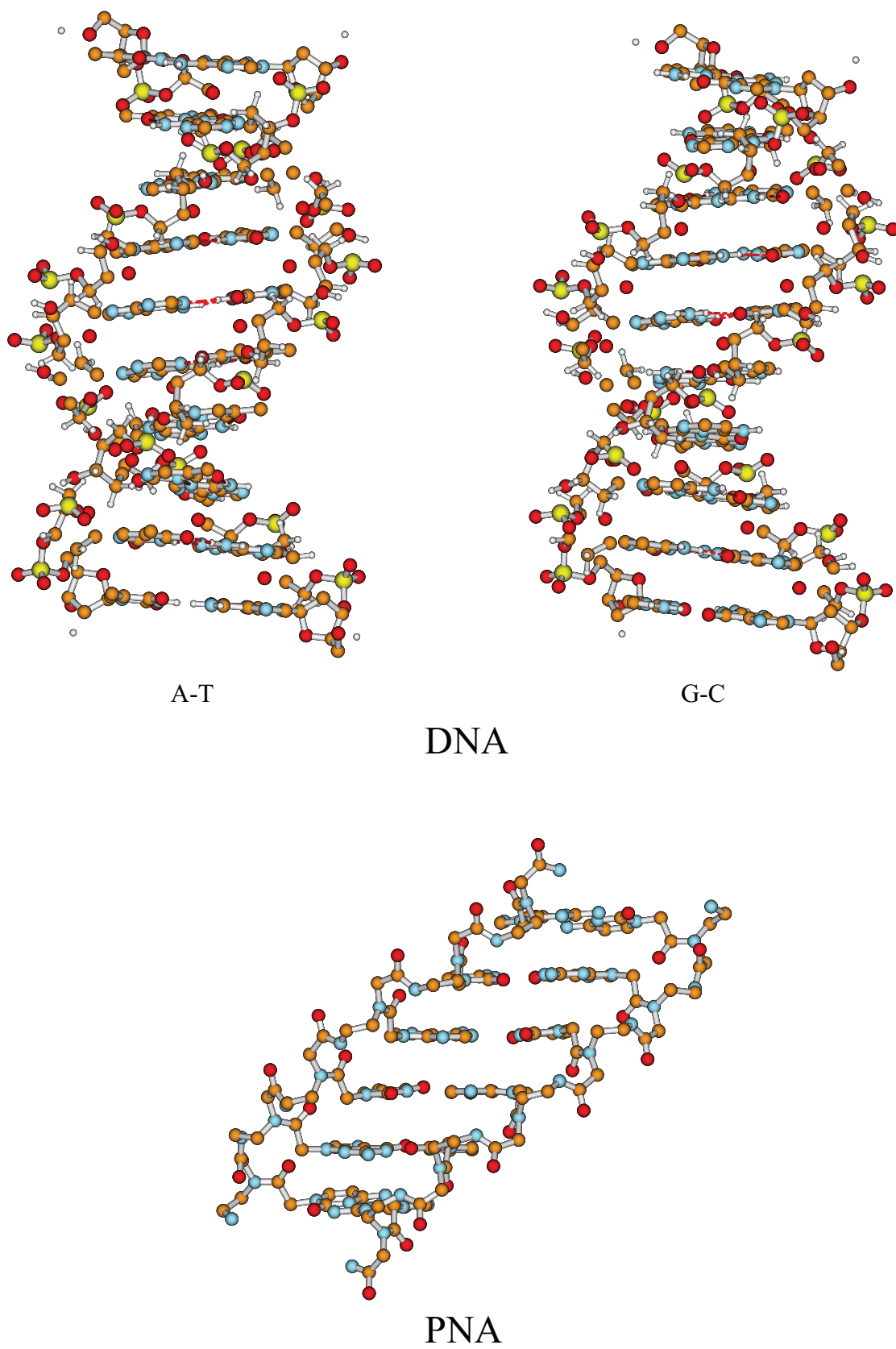


Figure 3.1: The structure of DNA and PNA.

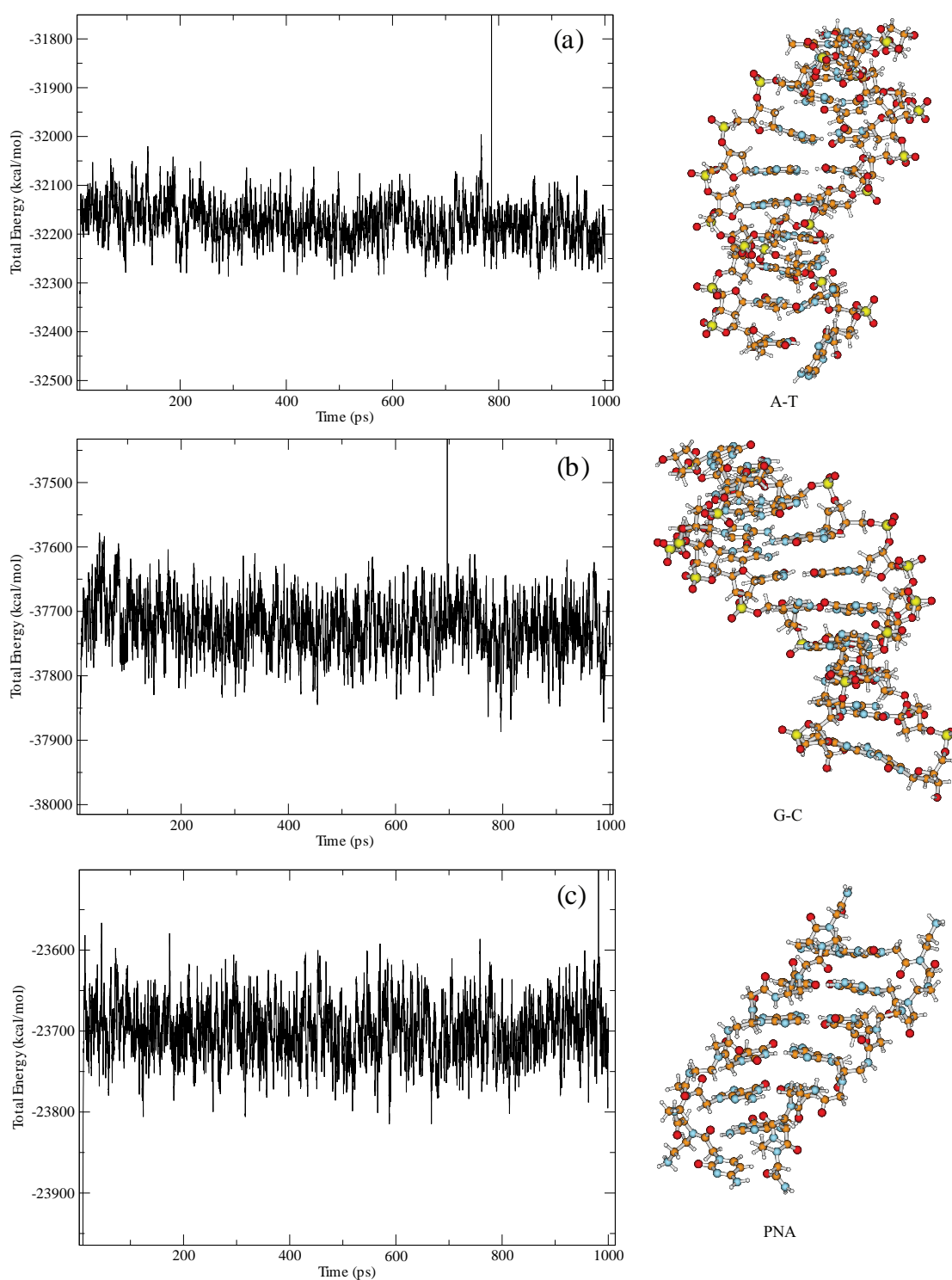


Figure 3.2: The graph shows the MD simulations results of DNA and PNA structures; (a) resulted graph of (AT) base pairs within DNA structure, (b) resulted graph of (GC) base pairs within DNA structure and (c) resulted graph of PNA structure

of the triangular Au plane is arranged in line with the $O \cdots H - N$ and $N \cdots H - N$ bonds of the corresponding base pairs. We placed the structures on the (x,y) plane and perpendicular to the z rotational axis in the Cartesian coordinate system. Then, we rotated the Au plane angle along the z axis and moved its plane to let its center of gravity superimposing with the center of gravity of the base by translation of (x,y) coordinate. The stacking distance was set at 3.2 \AA by translating on z axis. All structural patterns in this work were proposed according to the previous study by Y. Maeda et al [26]. For applying the electric field to all model structures, the point charges were utilized to each structure by stacking six triangularly-planar point charges above the Au(111) surface and below the base with opposite charges in same direction.

To investigate the effect of Au(111) on hydrogen bonds in the base pairs, all types of the terminal hydroxyl group at the asymmetric ends (5' and 3') for DNA systems were considered while PNA systems were considered only N-terminus because of the carboxyl group of C-terminus having a high steric effect with the Au plane. Single point calculations were performed using the 6-311++G(d,p) basis set for nucleic acid structures and LANL2DZ [43–45] basis set for Au(111) at B3LYP [46–48] level to generate the wave functions by Gaussian 03 program [49]. DFT methods [50–52] have been used for the hydrogen bonds systems, which are resulted by many researches [23–27, 40, 41, 53–55]. Besides, we selected 6-311++G(d,p) basis set for accurate results of molecules having a hydrogen bond. The resulting wave function was then analyzed by the atoms in molecules (AIM) formalism with the aid of AIM2000 program [56].

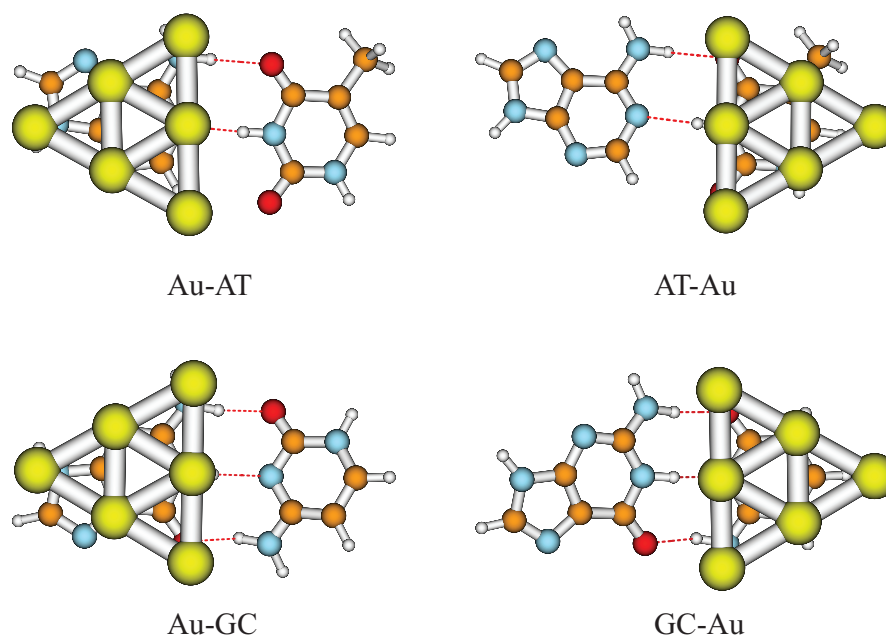


Figure 3.3: Model structures of the base pairs were stacked by Au(111).

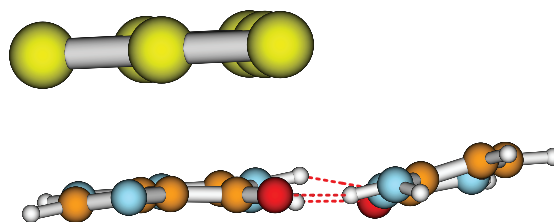


Figure 3.4: Detailed structure in the side view.

CHAPTER IV

RESULTS AND DISCUSSIONS

From the molecular graph of DNA and PNA geometries at central fragment obtained from the AIM analysis, the model structure of hydrogen bonds in the base pairs are illustrated in Figure 4.1. We considered the hydrogen bond interactions by the topological properties of the bond critical point (BCP) such as the electron density $\rho(r)$, the Laplacian of electron density $\nabla^2\rho(r)$, the ratio of the perpendicular contractions of ρ to its parallel expansion $|\lambda_1|/\lambda_3$, and the symmetry of the electron density distribution along the bond path (ellipticity, ε) [28]. The BCP of hydrogen bonds is classified in the category of closed-shell interactions, which have a relatively low value of ρ , positive $\nabla^2\rho$ and $|\lambda_1|/\lambda_3 < 1$ [57]. The strength of interaction can be described by the ellipticity value: decrease of ellipticity relate to a stronger interaction [16]. Also, the alteration of conformers can be explained by the change of bond paths, linked between two atoms via BCP [27,58,59].

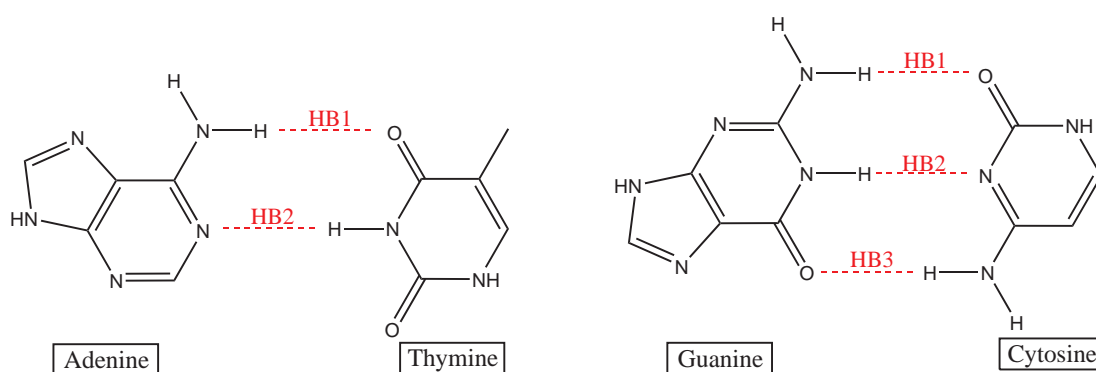


Figure 4.1: The definition of the positions of hydrogen bond interactions in base pairs.

4.1 Investigations of the effect of Au(111)

4.1.1 Topological properties of interaction analysis

The results of electron density topologies at BCPs originated on the hydrogen bonds between (AT) base pairs are presented in Figure 4.2 (Topological details are given in Table A1). The ellipticity change ($\% \Delta \epsilon$) in HB1 of A5'T3' conformers decrease more than A3'T5' in DNA structures, but this reduction is less than (AT) in PNA structures. These show a stronger effect of Au(111) on hydrogen bond interactions of the conformer A5'T3' than A3'T5' in DNA structures, but this effect is less than those incurred in (AT) of PNA structures. The ellipticity change of HB2 for A5'T3' conformers increased while that of A3'T5' decreased in higher quantities within DNA structures, but these changes are less than the decreasing within (AT) of PNA structures. These results indicated that the hydrogen bond interactions of A5'T3' conformers weaken less than the strengthening that occurred in A3'T5' conformers. But these effects are still lower than the strengthening within (AT) of PNA structures. Besides comparison of the ellipticity change between the stack of Au on (A) and (T) in DNA, the results show that the stacking of Au on (T) have a stronger effect than (A) in both H-bonds by 0.14% to 3.60%. In PNA, it has higher change in HB1 by 0.11% and lower change in HB2 by 0.22%. Therefore, the effects of Au stacking on (T) have more effective than (A) in both H-bonds. In PNA, they have more effective in HB1 but lower effective in HB2. Notwithstanding, the difference of the ellipticity change in this point have small value, which refer to the obtaining similar effect.

From Figure 4.3 (Topological details are given in Table A2), the changing ellipticity of (GC) base pairs in DNA at HB1 shows that ellipticity values of G5'C3' conformers increased while those of G3'C5' decreased in higher quantities. Whereas, these changes are less than the decreasing within (GC) of PNA structures. These indicate that the HB1 interactions in G5'C3' conformers weaken less than the strengthening of G3'C5', but also not as much as in PNA structures. At HB2, the decreasing ellipticity value of G5'C3' conformers are less than G3'C5' in DNA structures while the decreasing of (GC) in PNA structures is only greater than the

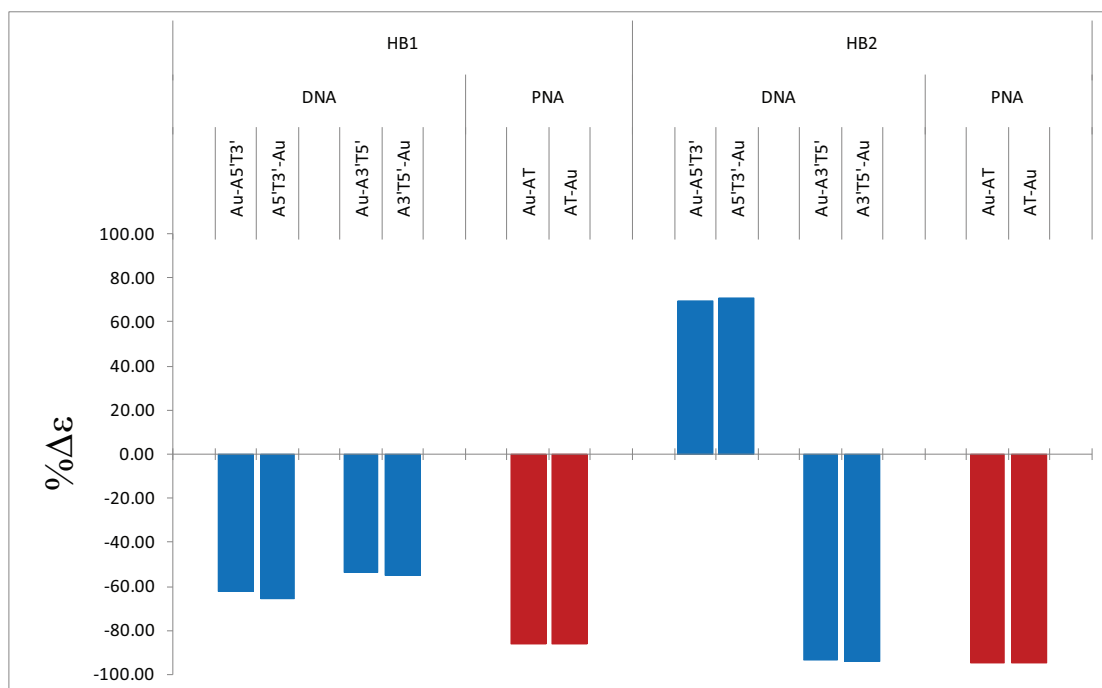


Figure 4.2: The ellipticity change of the hydrogen bond interactions between adenine (A) and thymine (T) base pairs.

G5'C3'-Au conformer. The results imply that the HB2 interactions of Au-G5'C3' and each G3'C5' conformers in DNA structures are stronger than (GC) in PNA structures which are stronger than G5'C3'-Au in DNA, and G3'C5' are affected the most. For HB3, the ellipticity change of G5'C3' conformers decrease less than G3'C5' in DNA structures, and (GC) conformers in PNA structures have the most decreasing. These indicated that the HB3 interactions of G5'C3' conformers strengthen less than G3'C5' in DNA structures, and represents the explicit distinction when compared to PNA structures that obtained the strongest effect. In DNA, the results show that the stacking of Au on (G) in G5'C3' conformers have larger change of $\% \Delta \epsilon$ than (C) in HB2 by 15.09% and HB3 by 1.75%, but lower change in HB1 by 3.84%. The reverse tendency of G3'C5' shows the differences of ellipticity change in HB1, HB2 and HB3 by 0.13%, 0.49% and 4.33%, respectively. These imply that the stacking of Au on (G) in G5'C3' conformers have more effective than (C) in HB2 and HB3, but less effective in HB1. The results of PNA show that the stacking of Au on (C) have a higher change of the ellipticity than (G) in all H-bonds by 0.34% to 2.45%, showing that the stacking of Au on (C) have more effective than (G) for all H-bonds.

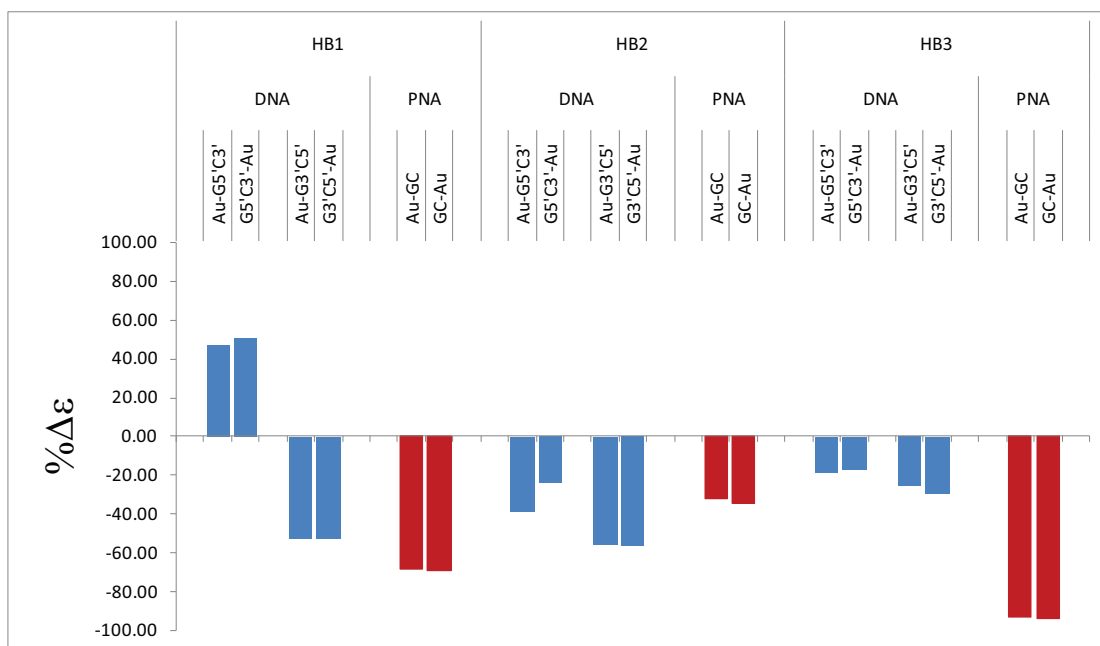


Figure 4.3: The ellipticity change of the hydrogen bond interactions between guanine (G) and cytosine (C) base pairs.

4.1.2 Topological properties of geometrical analysis

Table 4.1 showed the results of (AT) base pairs that the bond path lengths of HB1 increased while those of HB2 decreased in both A5'T3' and A3'T5' in DNA. For PNA, the bond path lengths of both H-bonds decreased. The results of (GC) base pairs in DNA indicate that the bond path lengths of all H-bonds in G5'C3' decreased while both HB1 and HB3 of G3'C5' conformers increased, but these lengths of HB2 decreased as illustrated in Table 4.2. Furthermore, PNA's results show a similar trend as G5'C3'.

Table 4.1: Bond path length (a.u.) of the $(3, -1)$ bond critical point (BCP) to each nuclei associated with the hydrogen bonds between adenine (A) and thymine (T) base pairs

structures		HB1			HB2		
		BCP-O	BCP-H	total	BCP-H	BCP-N	total
DNA	A5'T3'	2.3431	1.3792	3.7223	1.2461	2.2968	3.5429
	Au-A5'T3'	2.3876	1.3429	3.7305	1.1920	2.3257	3.5177
	A5'T3'-Au	2.3854	1.3449	3.7303	1.1903	2.3277	3.5179
	A3'T5'	2.6462	1.2408	3.8869	1.5534	2.7352	4.2886
	Au-A3'T5'	2.4549	1.4324	3.8873	1.3648	2.5313	3.8961
	A3'T5'-Au	2.4521	1.4351	3.8872	1.3614	2.5350	3.8964
PNA	AT	2.6708	0.8353	3.5061	1.4455	2.1874	3.6328
	Au-AT	2.2214	1.2008	3.4222	1.2004	2.3314	3.5318
	AT-Au	2.2224	1.1998	3.4222	1.2010	2.3309	3.5319

Table 4.2: Bond path length (a.u.) of the $(3, -1)$ bond critical point (BCP) to each nuclei associated with the hydrogen bonds between guanine (G) and cytosine (C) base pairs

structures		HB1			HB2			HB3		
		BCP-O	BCP-H	total	BCP-N	BCP-H	total	BCP-H	BCP-O	total
DNA	G5'C3'	2.2299	1.2634	3.4933	2.2392	1.5281	3.7674	1.1231	2.2882	3.4112
	Au-G5'C3'	2.2084	1.1956	3.4040	2.3952	1.2904	3.6856	1.1408	2.1574	3.2982
	G5'C3'-Au	2.2075	1.1964	3.4039	2.3925	1.2924	3.6849	1.1397	2.1586	3.2983
	G3'C5'	2.4076	1.2635	3.6711	2.3671	1.4357	3.8028	1.3237	2.4548	3.7785
	Au-G3'C5'	2.3450	1.3409	3.6859	2.4556	1.3114	3.7670	1.3900	2.3972	3.7872
	G3'C5'-Au	2.3420	1.3434	3.6854	2.4525	1.3142	3.7667	1.3881	2.3995	3.7875
PNA	GC	2.3210	1.2505	3.5715	2.5390	1.6216	4.1606	1.5266	2.7420	4.2686
	Au-GC	2.2904	1.2729	3.5633	2.6414	1.4750	4.1164	1.5667	2.6844	4.2511
	GC-Au	2.2919	1.2714	3.5633	2.6431	1.4734	4.1165	1.5686	2.6824	4.2509

Figure 4.4 shows a representative of the occurred differences in the molecular orbital (MO) that involved with hydrogen bonds between (AT) base pair in DNA which have the similar appearances as the isolated structure and the structure combined with Au(111). The density of state (DOS) profiles of their structure in Figure 4.5 manifest the change that occurred when the base pair structure was combined with Au(111). Furthermore, Figure 4.6 exhibits the MO energy profiles obtained from the structure system shown in Figure 4.4, which have a decreasing trend and augmentation of MOs involved with hydrogen bonds when the structure was stacked by Au(111).

From all of the aforementioned results, we found that the results of topological properties from HB2 in (GC) base pairs manifested the different trend of the ellipticity change between DNA and PNA when compared with other H-bonds. This is presumably, because the hydrogen atoms at the position of hydrogen bond interactions in (GC) base pairs within DNA backbone have a chance to establish the proton transfer, if they are in transition state which is most active at N...H position [53,54]. Moreover, the conformers of G5'C3' in DNA displayed the significant difference of the ellipticity change at HB2 when Au(111) stacks on different base. This is presumptive that not only the occurrence of the proton transfer process on the hydrogen bond interactions at N...H position, but also having the effect from the electron-donor and acceptor properties of purines and pyrimidines bases. Generally, the purines base qualify as an electron-acceptor while it is a better electron-donor and chemical reactive than the pyrimidines base [60–62]. Then, the analysis of the electron density had shown that all structure systems satisfied the designative criteria of hydrogen bond interactions. The change of DOS and MOs confirms that Au affects the structural change and also leads to the overall interactions strengthening.

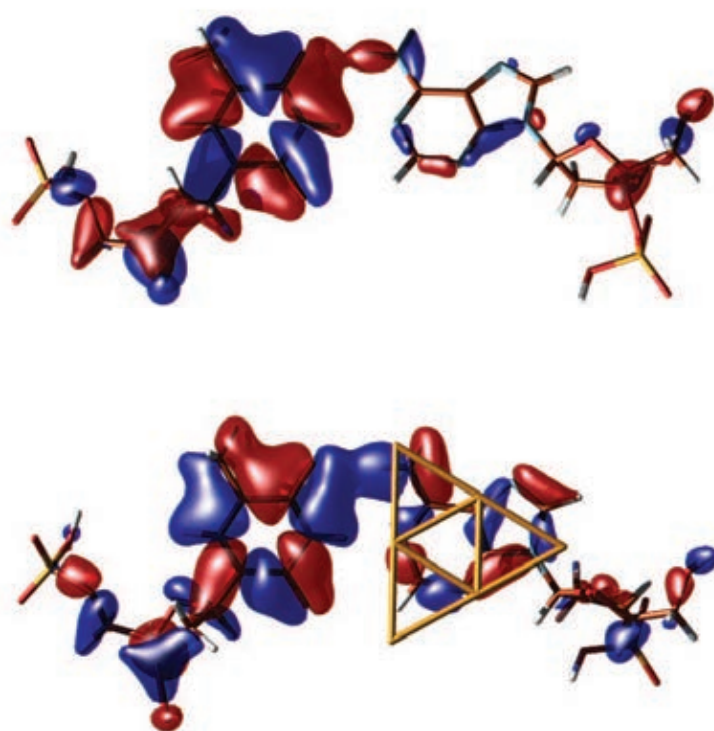


Figure 4.4: The representative of the molecular orbitals of the isolated structure and the structure combined with Au(111) that involved with the hydrogen bonds.

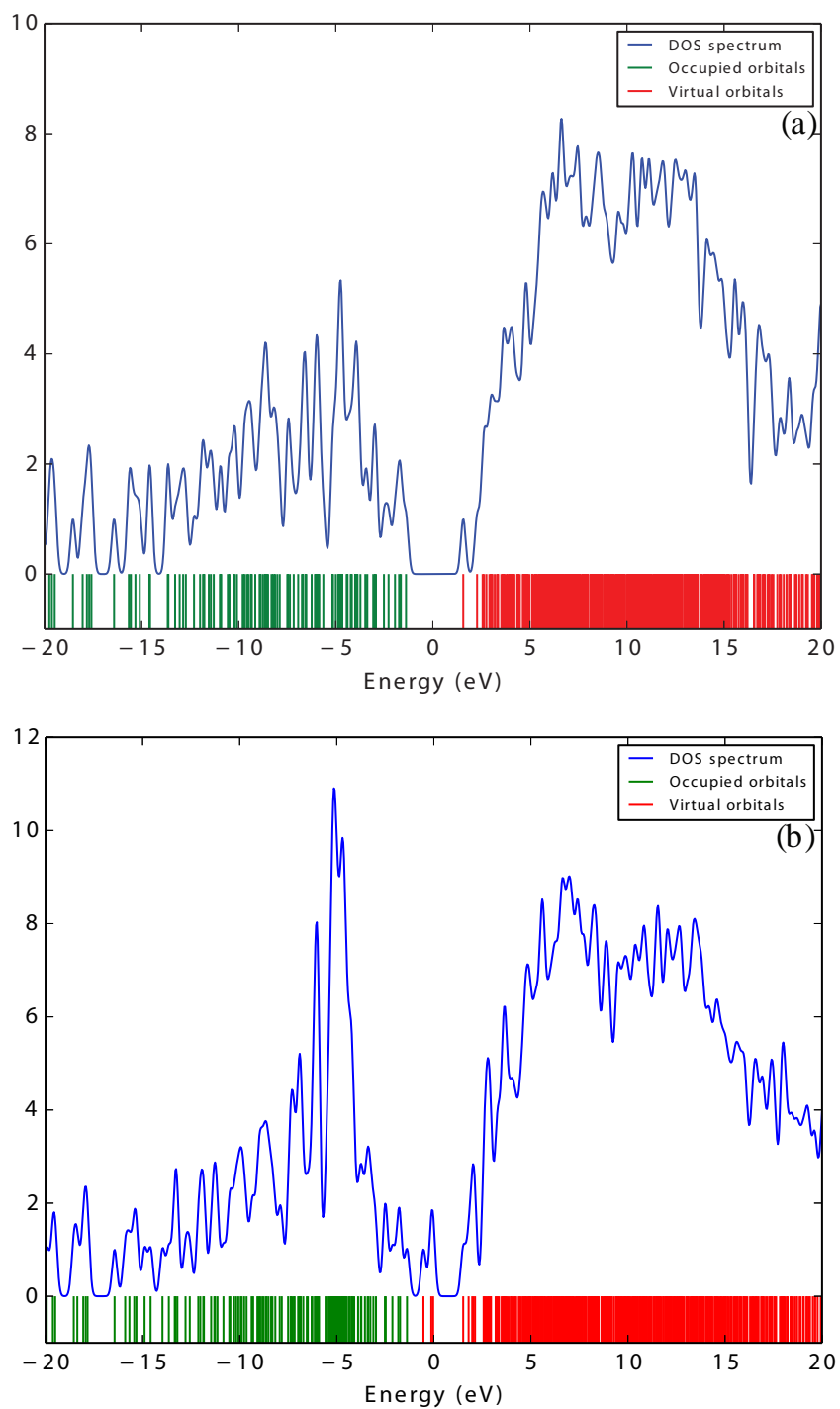


Figure 4.5: The density of state profiles of (a) the isolated structure and (b) the structure combined with Au(111).

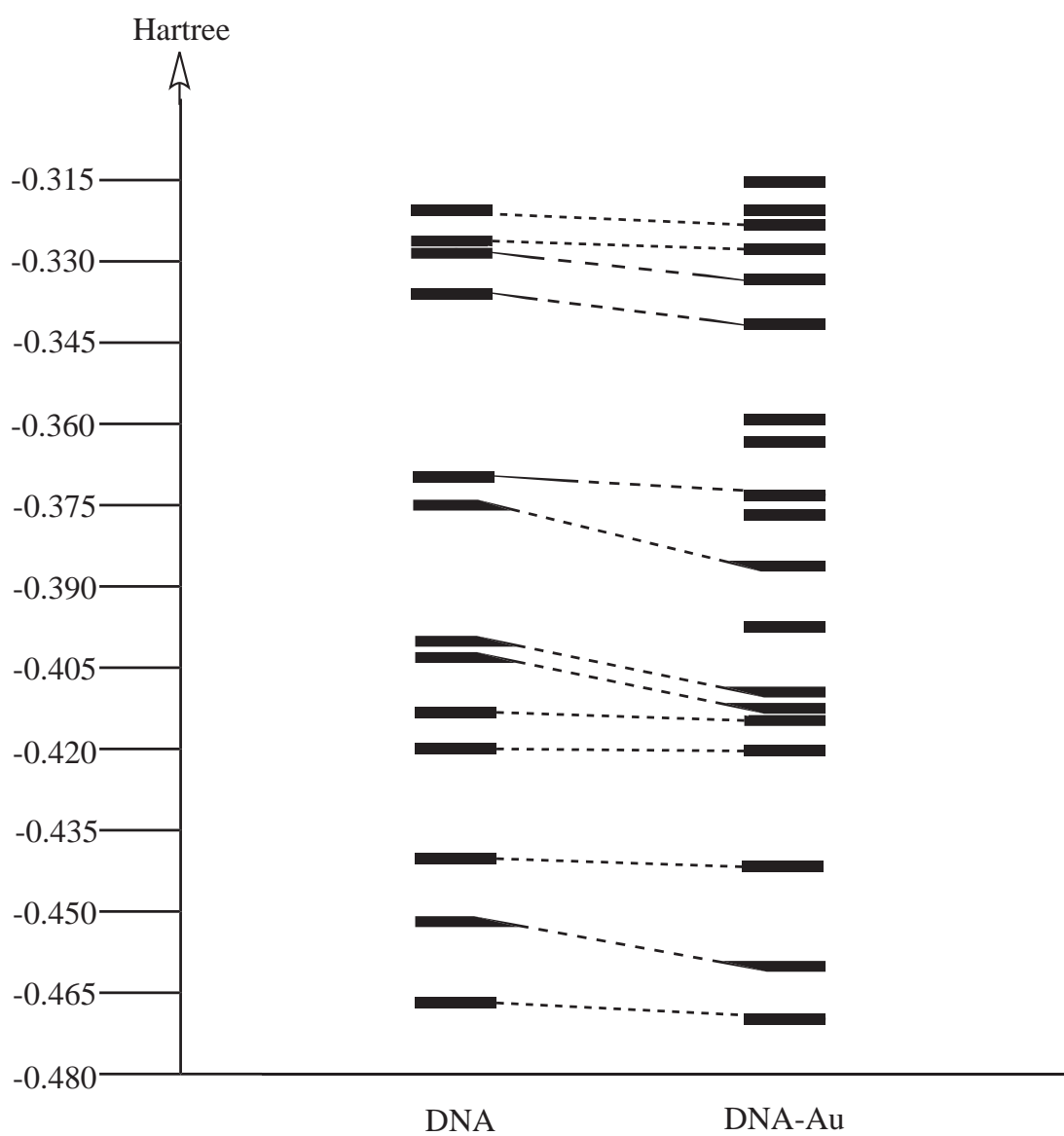


Figure 4.6: The molecular orbitals energy profiles of the isolated structure and the structure combined with Au(111) that involved with the hydrogen bonds.

4.2 Investigations of the electric field effect on complex structures

4.2.1 Topological properties of interaction analysis

Figure 4.7 (Topological details are given in Table A3) revealed the tendency of $\% \Delta \epsilon$ when the complex structure of (AT) base pairs were applied in the electric field by point charge size of 0.1, 0.2, and 0.3, respectively, some ellipticity give a result of the different value change at the fifth decimal place from now on. At HB1, the results show that only A5'T3'-Au conformer of DNA has a decreasing trend in ascending order of point charge values, and an increasing trend when the direction of electric field was alternated. These indicate that the HB1 interactions in A5'T3'-Au conformer strengthen depending on the electric field intensity when the electron density was induced from the base pair toward the Au(111). But, it weaken depending on the electric field intensity when the electron density was induced from the Au(111) toward the base pair. On the other hand, the results show that only AT-Au conformer of PNA has a decreasing trend in ascending order of point charge values, even though the electric field direction was alternated. These imply that the HB1 interactions in AT-Au conformer strengthen depending on the electric field intensity, but it is independent of the direction of the electron density induction. Besides, the results exhibit that the Au-A5'T3' conformer within DNA has an increasing trend in ascending order of point charge values in only case of the electric field was applied by stacking the positive charges above the Au(111) surface and negative charges under the base. On the contrary, Au-A3'T5' within DNA and Au-AT within PNA conformers have a decreasing trend in ascending order of point charge values in only case of the electric field was applied by stacking the negative charges above the Au(111) surface and positive charges under the base. These indicate that the HB1 interactions in Au-A5'T3' conformer weaken depending on the electric field intensity in only case of the electron density induced from the base pair toward the Au(111), while the HB1 interactions in Au-A3'T5' and Au-AT conformers strengthen depending on the electric field intensity in only case of the electron density induced from the Au(111) toward the base pair. In A3'T5'-Au

conformer within DNA, the results cannot be identified a trend. For HB2 results, there are Au-A5'T3' and A3'T5'-Au conformers of DNA, and AT-Au conformer of PNA. They have the decreasing trends in the ascending order of point charge values and the increasing trends when the direction of electric field was reversed, while A5'T3'-Au conformer of DNA displays the contrary results. These imply that the HB2 interactions in Au-A5'T3', A3'T5'-Au and AT-Au conformers strengthen depending on the electric field intensity when the electron density was induced from the base pair toward the Au(111). But, they weaken depending on the electric field intensity when the electron density was induced from the Au(111) toward the base pair. On the other hand, the HB2 interactions in A5'T3'-Au conformer weaken depending on the electric field intensity when the electron density was induced from the base pair toward the Au(111). But, it strengthen depending on the electric field intensity when the electron density was induced from the Au(111) toward the base pair. Withal, the results display that the Au-AT conformer within PNA has a decreasing trend in ascending order of point charge values in only case of the electric field by stacking positive charges above the Au(111) surface and negative charges under the base. These imply that the HB2 interactions in Au-AT conformer strengthen depending on the electric field intensity in only case of the electron density induced from the base pair toward the Au(111). In Au-A3'T5' conformer within DNA, the results do not give a definite trend.

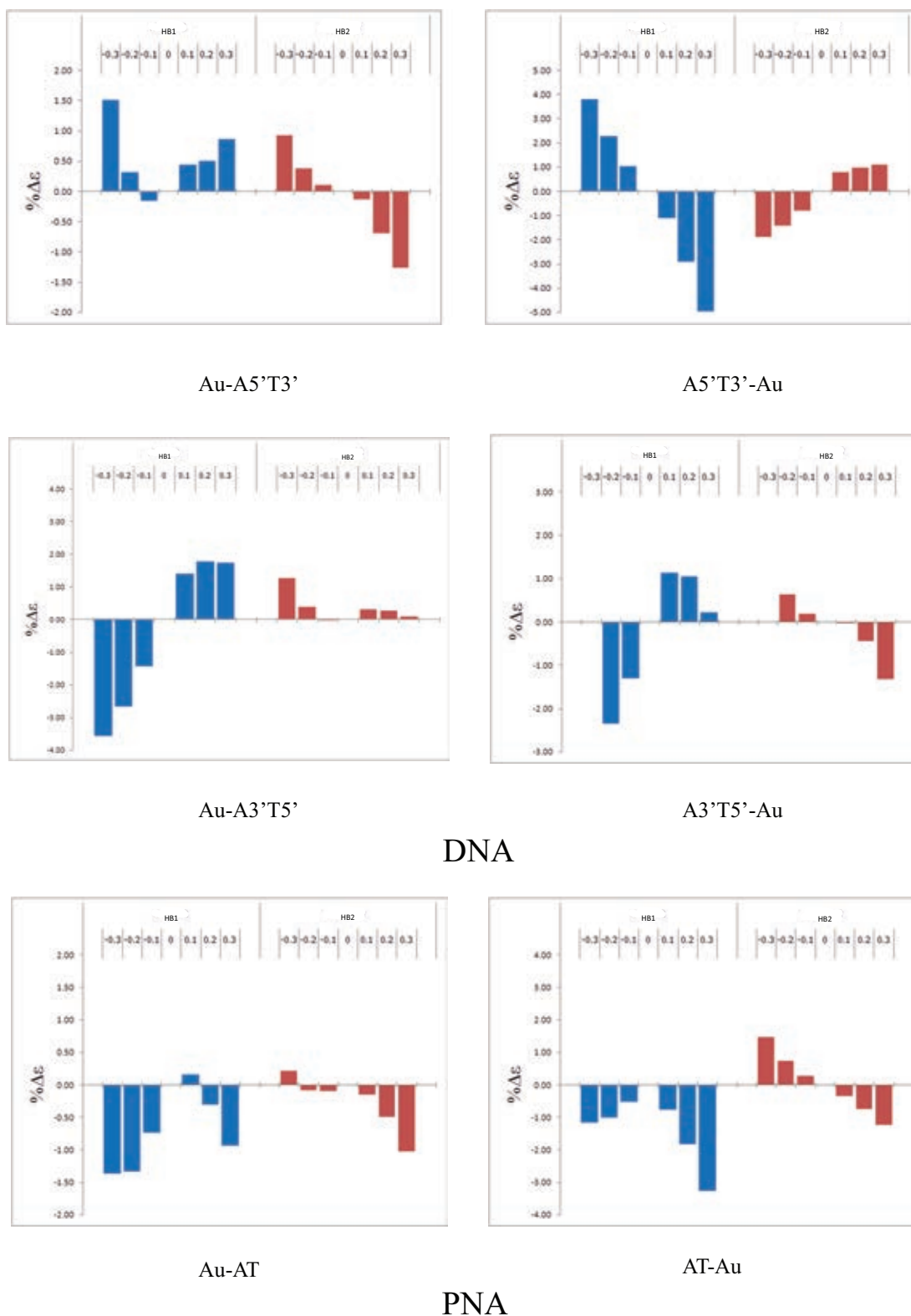
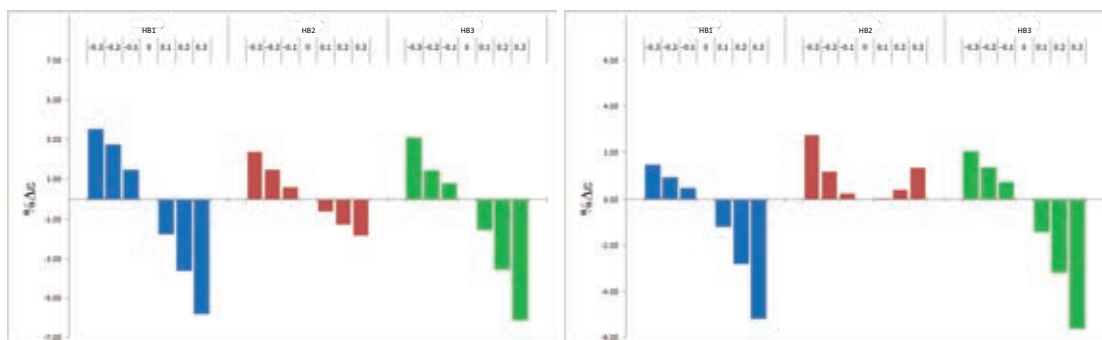


Figure 4.7: The tendency of ellipticity change of the hydrogen bond interactions between adenine (A) and thymine (T) base pairs.

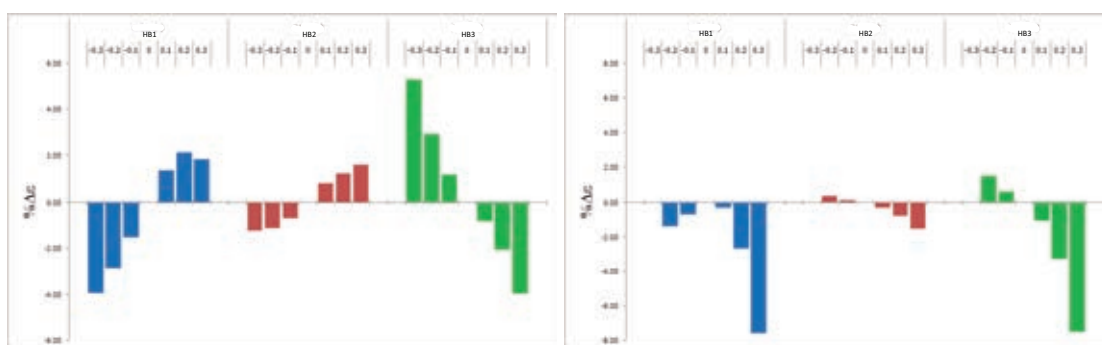
From Figure 4.8 (Topological details are given in Table A4), the tendency of ellipticity change of (GC) base pairs at HB1 shows that Au-G5'C3' and G5'C3'-Au conformers of DNA have the decreasing trends in the ascending order of point charge values, and the increasing trends when the direction of electric field was alternated. The results indicate that the HB1 interactions in Au-G5'C3' and G5'C3'-Au conformers strengthen depending on the electric field intensity when the electron density was induced from the base pair toward the Au(111). But, they weaken depending on the electric field intensity when the electron density was induced from the Au(111) toward the base pair. On the one hand, the results exhibit that G3'C5'-Au conformer of DNA has a decreasing trend in the ascending order of point charge values, even if the electric field direction was reversed. These imply that the HB1 interactions in G3'C5'-Au conformer strengthen depending on the electric field intensity, but it is independent of the direction of the electron density induction. Besides, the results show that both Au-G3'C5' within DNA and GC-Au within PNA conformers have a decreasing trend in ascending order of point charge values in only case of the electric field applied by stacking negative charges above the Au(111) surface and positive charges under the base. On the other side, Au-GC conformer within PNA has a decreasing trend in ascending order of point charge values in only case of the electric field applied by stacking positive charges above the Au(111) surface and negative charges under the base. These indicate that the HB1 interactions in both Au-G3'C5' and GC-Au conformers strengthen depending on the electric field intensity in only case of the electron density induced from the Au(111) toward the base pair, while the HB1 interactions in Au-GC conformer strengthen depending on the electric field intensity in only case of the electron density induced from the base pair toward the Au(111). For HB2 results, there are Au-G5'C3' and G3'C5'-Au conformers of DNA, and Au-GC conformer of PNA. They have the decreasing trends in the ascending order of point charge values, and the increasing trends when the direction of electric field was alternated. On the contrary, the Au-G3'C5' conformer of DNA displays the adverse results. These indicate that the HB2 interactions in Au-G5'C3', G3'C5'-Au and Au-GC conformers strengthen depending on the electric field intensity when the electron density was induced from the base pair toward the Au(111). But, they weaken depending on the electric field intensity when the electron density was induced from the Au(111) toward the base pair. On

the other hand, the HB2 interactions in Au-G3'C5' conformer weaken depending on the electric field intensity when the electron density was induced from the base pair toward the Au(111). But, it strengthens depending on the electric field intensity when the electron density was induced from the Au(111) toward the base pair. Moreover, the results display that G5'C3'-Au conformer of DNA has an increasing trend in the ascending order of point charge values, although the electric field direction was alternated. These imply that the HB2 interactions in G5'C3'-Au conformer weaken depending on the electric field intensity, but it is independent of the direction of the electron density induction. Withal, the results show that GC-Au conformer within PNA has an increasing trend in ascending order of point charge values in only case of the electric field applied by stacking positive charges above the Au(111) surface and negative charges under the base. These indicate that the HB2 interactions in GC-Au conformer weaken depending on the electric field intensity in only case of the electron density induced from the base pair toward the Au(111). At HB3, the results manifest that all conformers of DNA and Au-GC conformer of PNA have the decreasing trends in the ascending order of point charge values, and the increasing trends when the direction of electric field was reversed. These indicate that the HB3 in all DNA conformers and Au-GC conformer strengthens depending on the electric field intensity when the electron density was induced from the base pair toward the Au(111). But, they weaken depending on the electric field intensity when the electron density was induced from the Au(111) toward the base pair. Furthermore, the results display that GC-Au conformer within PNA has a decreasing trend in ascending order of point charge values in only case of the electric field applied by stacking positive charges above the Au(111) surface and negative charges under the base. These imply that the HB3 interactions in GC-Au conformer strengthen depending on the electric field intensity in only case of the electron density induced from the base pair toward the Au(111).



Au-G5'C3'

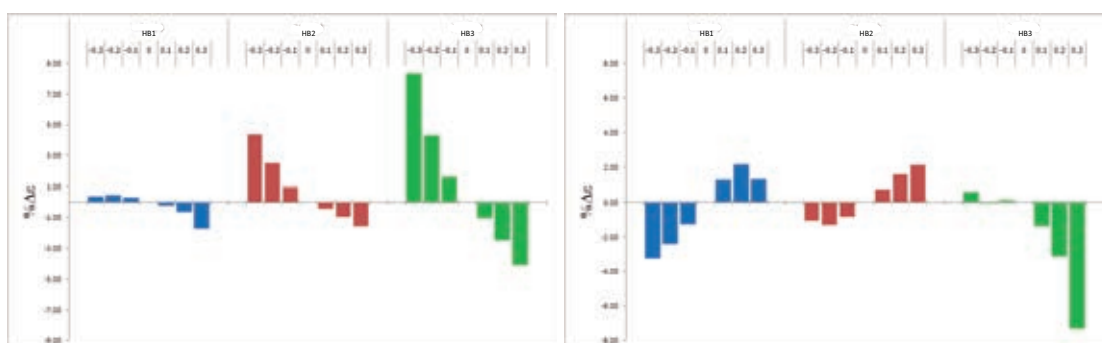
G5'C3'-Au



Au-G3'C5'

G3'C5'-Au

DNA



Au-GC

GC-Au

PNA

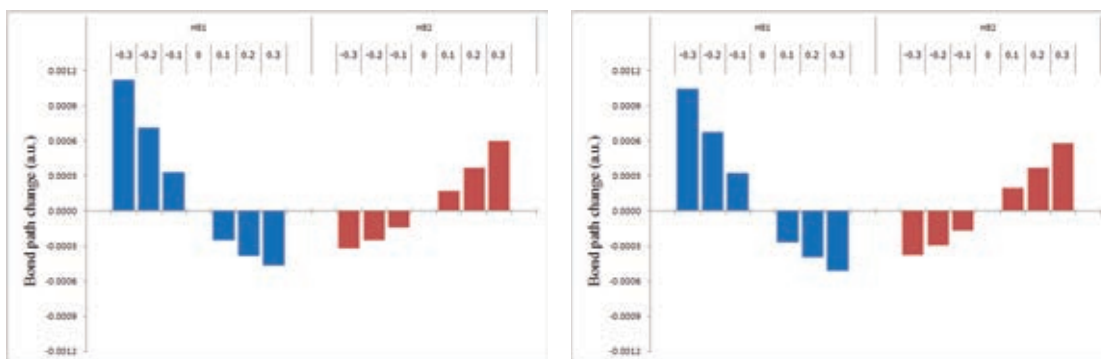
Figure 4.8: The tendency of ellipticity change of the hydrogen bond interactions between guanine (G) and cytosine (C) base pairs.

According to the results of Figure 4.7 and Figure 4.8, we could calculate the effect of electric field on hydrogen bonds in A3'T5'-Au and G3'C5'-Au conformers of DNA by the point charge size of 0.3 in only one direction. These indicated the calculations of conformers that Au stacks on pyrimidine bases at the 5'-terminal position in DNA, which are significantly affected. Furthermore, we can classify the tendency into four types. First, the decreasing or increasing in the ascending order of point charge values hinges on the electric field direction. Second, the decreasing or increasing in the ascending order of point charge values depend on the electric field in one direction. Third, the decreasing or increasing in the ascending order of point charge values is independent of the electric field direction. Finally, the change cannot be identified a trend.

4.2.2 Topological properties of geometrical analysis

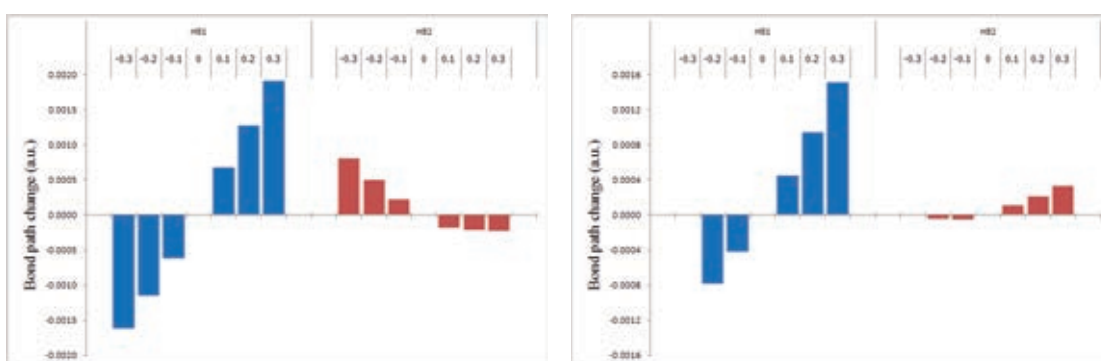
Figure 4.9 (Bond path details are given in Table A5) represents the tendency of bond path lengths when the complex structures of (AT) base pairs were applied in the electric field by point charge size of 0.1, 0.2, and 0.3, respectively. The Au-A5'T3' and A5'T3'-Au conformers of DNA show that the bond path lengths of HB1 have a decreasing trend in ascending order of point charge values, and increasing trend when alternate the electric field direction while HB2 shows the contrary results. In Au-A3'T5' conformer of DNA, the results of bond path lengths show the opposite trend to Au-A5'T3' and A5'T3'-Au conformers while A3'T5'-Au conformer shows an increasing trend in the ascending order of point charge values, and a decreasing trend when alternate the electric field direction in both H-bonds. For PNA, the results of Au-AT conformer show that HB1 have an increasing trend in ascending order of point charge values in only case of the electric field applied by stacking negative charges above the Au(111) surface and positive charges under the base. On the other hand, the HB2 shows an increasing trend in the ascending order of point charge values, and a decreasing trend when alternate the electric field direction. In AT-Au conformer, the results of bond path lengths show the same trend as Au-A3'T5' conformer of DNA.

In Figure 4.10 (Bond path details are given in Table A6), the results of (GC) base pairs within DNA exhibit that the bond path lengths of both HB1 and HB3 in Au-G5'C3' and G5'C3'-Au conformers have the same increasing trend in the ascending order of point charge values, and a decreasing trend when reverse the electric field direction. But, Au-G3'C5' conformer displays the same trend in both HB1 and HB2, which are opposite to HB3. Moreover, G3'C5'-Au conformer shows that the bond path lengths of HB2 have an increasing trend in ascending order of point charge values, and decreasing trend when alternate the electric field direction. On the other hand, HB1 has an increasing trend in ascending order of point charge values, even though the electric field direction was alternated. For PNA, the results of Au-GC conformer represent that the bond path lengths of HB1 have an increasing trend in ascending order of point charge values in only case of the electric field applied by stacking positive charges above the Au(111) surface and negative charges under the



Au-A5'T3'

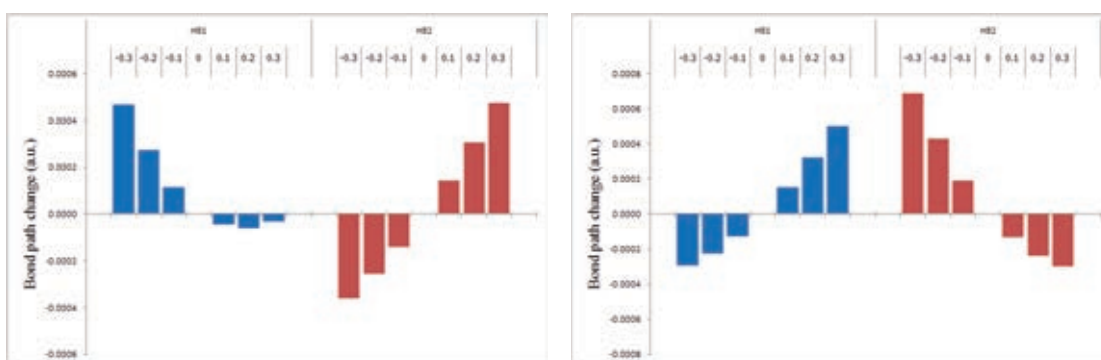
A5'T3'-Au



Au-A3'T5'

A3'T5'-Au

DNA



Au-AT

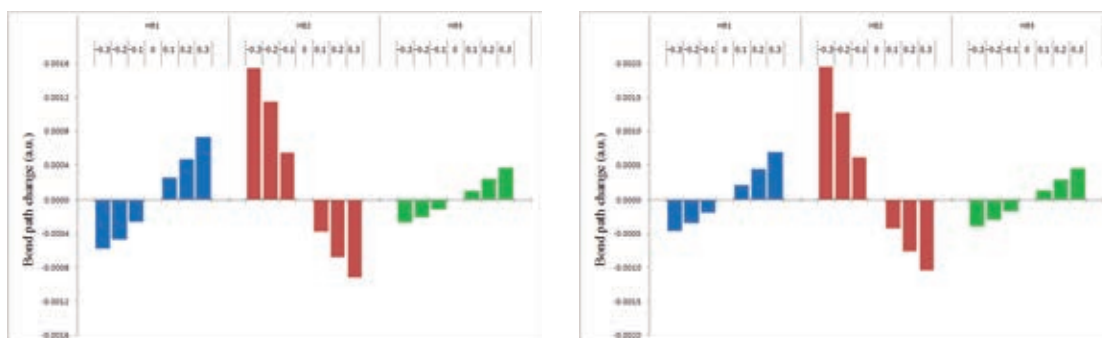
AT-Au

PNA

Figure 4.9: The tendency of bond path change of the hydrogen bond interactions between adenine (A) and thymine (T) base pairs.

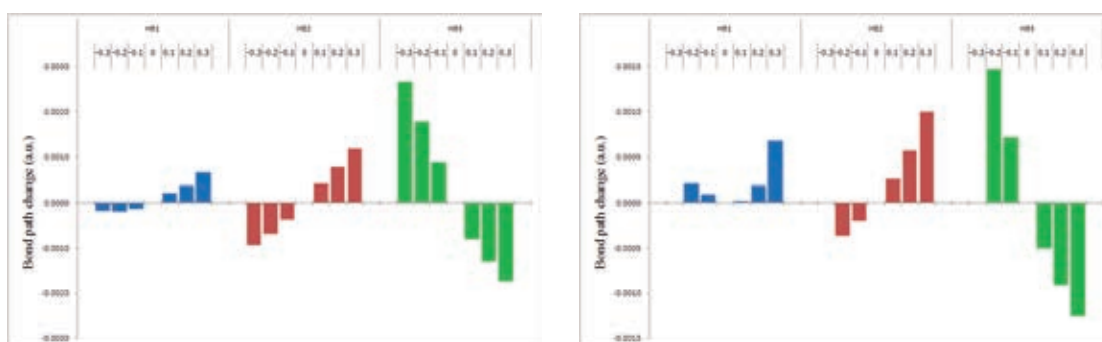
base. On the other side, the GC-Au conformer shows the increasing trend in ascending order of point charge values in only case of the electric field applied by stacking negative charges above the Au(111) surface and positive charges under the base. In HB2, all conformers display that the bond path lengths have an increasing trend in ascending order of point charge values, although the electric field direction was alternated. But, HB3 of Au-GC conformer has a decreasing trend in ascending order of point charge values, and increasing trend when alternate the electric field direction.

From all of the bond path results contained herein, we can classify the bond path change tendency into three types. First, the change depend on the electric field intensity and direction. Second, the change depend on the intensity of electric field in one direction. Finally, the change depend on the electric field intensity but independent of the electric field direction.



Au-G5'C3'

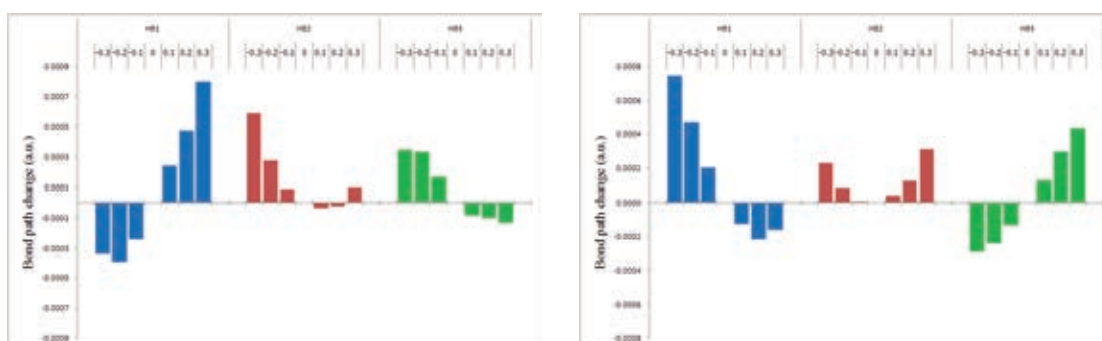
G5'C3'-Au



Au-G3'C5'

G3'C5'-Au

DNA



Au-GC

GC-Au

PNA

Figure 4.10: The tendency of bond path change of the hydrogen bond interactions between guanine (G) and cytosine (C) base pairs.

4.2.3 Electronic properties investigation on complex structures

Figure 4.11 shows the energy gap profiles of the base pair structures combined with Au(111) (see details in Table A7), applying in the electric field. The results of the structures before being applied by the electric field represent the energy gap in both DNA and PNA of the complex structures that the (AT) is higher than (GC) base pair. These explain that the (GC) base pair within the nucleic structure has an electrical conductivity greater than the (AT) base pair, in agreement with the theoretical study of Tsukamoto et al. [40] and the experimental results of Xu et al. [63]. The energy gap of DNA is higher than PNA, indicating that the latter structure has an electrical conductivity greater than the former. Then, we considered the results of the structures without the electric field compare with those within electric field. These exhibit that the energy gap decreases when the electron density was induced from the base pair toward the Au(111). On the contrary, it increases when the electron density was induced from the Au(111) toward the base pair, but this energy gap drops when increasing the electric field intensity toward the point charges size at 0.3. The results imply that the electrical conductivity of all structures behave as an insulator at low bias, and become conductor when the voltage applied across it exceeds the breakdown voltage. These suggest that all structures can be semiconductor to conductor, in agreement with the experimental data of Porath et al. [64] and Xu et al. [65].

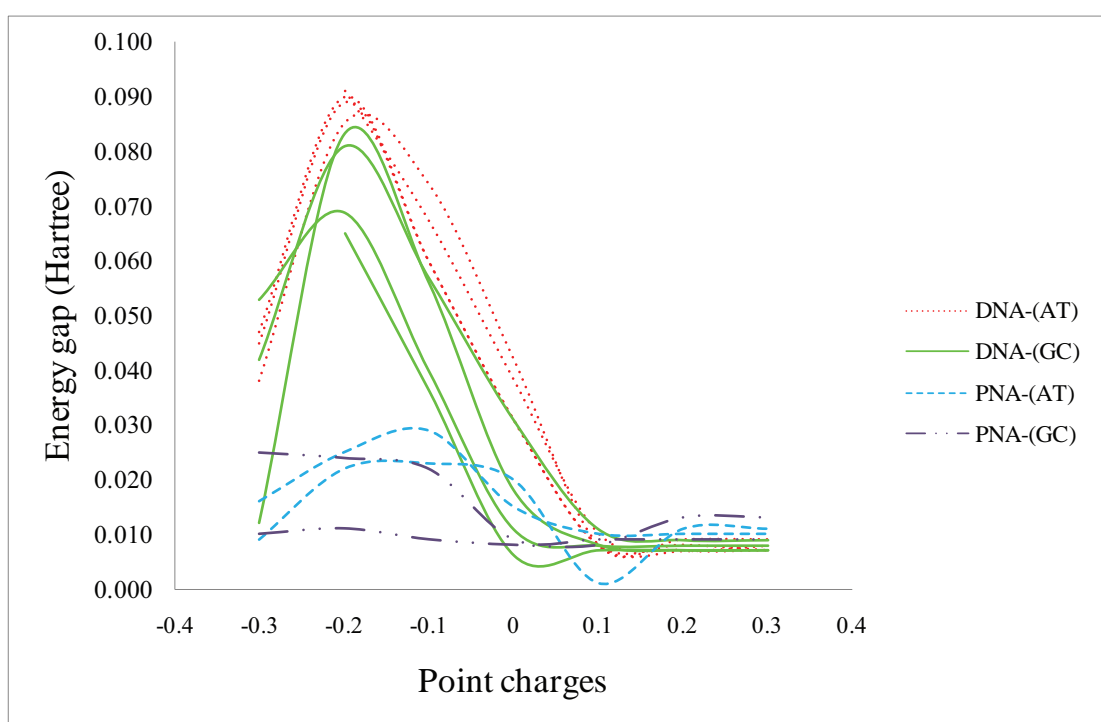


Figure 4.11: Energy gap profiles of the base pair structures combined with Au(111) were applied in the electric field.

CHAPTER V

CONCLUSION

In this research, we employed topologies at bond critical point according to the AIM theory, investigating the effect of Au(111) on hydrogen bond in DNA and PNA base pairs. The results indicated that the hydrogen bond interactions within the PNA structures gain a stronger effect than DNA except N \cdots H of (GC) base pairs. The tendency of the effect when stacking Au(111) on either purine or pyrimidine bases is similar, excepting N \cdots H of G5'C3' conformers in DNA which differ significantly. PNA gain a stronger effect from Au(111) and has the similar trends while the tendency of DNA is high variability. For the alteration of conformers, the results elucidated that PNA have the same tendencies in all structures while those in DNA have a high variability. The effect results of the structures within an electric field exhibit four categories of the ellipticity and the bond path change tendency, which are a trend that depend on the electric field intensity and direction, a trend that depend on the intensity of electric field in one direction, a trend that depend on the electric field intensity but independent of the electric field direction, and a trend that cannot be classified. The energy gap profiles imply that the (GC) base pair has an electrical conductivity greater than the (AT) base pair within nucleic structures, and PNA structures manifest the electrical conductivity that is greater than DNA structures. In addition, the electrical conductivity behaviors of all structures resemble a conductor. From all of the above reason, these can be apply and develop the molecular devices by controlling the properties of hydrogen bonds and structural change. Moreover, the effect on the structures within an electric field shows that the change tendency of the hydrogen bond interactions, the structures and the electrical conductivity behaviors, which can be applied for establishing the electrical conductor from nucleic structures [64,66], and the knowledge of the molecular logic gates [67].

REFERENCES

- [1] P. E. Nielsen, M. Egholm, R. H. O. Buchardt *Sequence-selective recognition of DNA by strand displacement with a thymine-substituted polyamide* *Science*, **1991**, 254, 1497–1500.
- [2] C. Hélène, J.-J. Toulmé *Specific regulation of gene expression by antisense, sense and antigene nucleic acids* *BBA-Gene Struct. Expr.*, **1990**, 1049, 99–125.
- [3] E. Uhlmann, A. Peyman *Antisense oligonucleotides: a new therapeutic principle* *Chem. Rev.*, **1990**, 90, 543–584.
- [4] P. Nielsen, M. Egholm, O. Buchardt *Peptide nucleic acid (PNA). A DNA mimic with a peptide backbone* *Bioconjugate Chem.*, **1994**, 5, 3–7.
- [5] P. E. Nielsen, M. Egholm, O. Buchardt *Sequence-specific transcription arrest by peptide nucleic acid bound to the DNA template strand* *Gene*, **1994**, 149, 139–145.
- [6] J. C. Hanvey, N. J. Peffer, J. E. Bisi, S. A. Thomson, R. Cadilla, J. A. Josey, D. J. Ricca, C. F. Hassman, M. A. Bonham, K. G. Au, S. G. Carter, D. A. Bruckenstein, A. L. Boyd, S. A. Noble, L. E. Babiss *Antisense and antigene properties of peptide nucleic acids* *Science*, **1992**, 258, 1481–1485.
- [7] M. Egholm, O. Buchardt, L. Christensen, C. Behrens, S. M. Freier, D. A. Driver, R. H. Berg, S. K. Kim, B. Norden, P. E. Nielsen *PNA hybridizes to complementary oligonucleotides obeying the Watson–Crick hydrogen-bonding rules* *Nature*, **1993**, 365, 566–568.
- [8] V. V. Demidov, V. N. Potaman, M. Frank-Kamenetskii, M. Egholm, O. Buchardt, S. H. Sönnichsen, P. E. Nielsen *Stability of peptide nucleic acids in human serum and cellular extracts* *Biochem. Pharmacol.*, **1994**, 48, 1310–1313.
- [9] M. A. Bonham, S. Brown, A. L. Boyd, P. H. Brown, D. A. Bruckenstein, J. C. Hanvey, S. A. Thomson, A. Pipe, F. Hassman, J. E. Bisi, B. C. Froehler, M. D. Matteucci, R. W. Wagner, S. A. Noble, L. E. Babiss *An assessment of the antisense properties of RNase H-competent and steric-blocking oligomers* *Nucleic Acids Res.*, **1995**, 23, 1197–1203.

- [10] H. Knudsen, P. E. Nielsen *Antisense Properties of Duplex- and Triplex-Forming PNAs* *Nucleic Acids Res.*, **1996**, *24*, 494–500.
- [11] U. Koppelhus, P. E. Nielsen *Cellular delivery of peptide nucleic acid (PNA)* *Adv. Drug Deliv. Rev.*, **2003**, *55*, 267–280.
- [12] P. E. Nielsen, M. Egholm *An Introduction to PNA*; Taylor & Francis Routledge: England, 2004.
- [13] T. Ratilainen, A. Holmén, E. Tuite, G. Haaima, L. Christensen, P. E. Nielsen, B. Nordén *Hybridization of Peptide Nucleic Acid* *Biochemistry*, **1998**, *37*, 12331–12342.
- [14] T. Ratilainen, A. Holmén, E. Tuite, P. E. Nielsen, B. Nordén *Thermodynamics of Sequence-Specific Binding of PNA to DNA* *Biochemistry*, **2000**, *39*, 7781–7791.
- [15] P. Nielsen *PNA technology* *Molecular Biotechnology*, **2004**, *26*, 233–248.
- [16] S. Jalili, H. Aghdastinat *Study of hydrogen bonding in dihydroxyacetone and glyceraldehyde using computational methods* *J. Mol. Struct.: THEOCHEM*, **2008**, *857*, 7–12.
- [17] F. J. Luque, J. M. López, M. López de la Paz, C. Vicent, M. Orozco *Role of Intramolecular Hydrogen Bonds in the Intermolecular Hydrogen Bonding of Carbohydrates* *J. Phys. Chem. A*, **1998**, *102*, 6690–6696.
- [18] P. Hobza, C. Sandorfy *A quantum chemical study of the effect of Na⁺ on the hydrogen bonds in the adenine-thymine base-pair* *Biophys. Chem.*, **1984**, *19*, 201–209.
- [19] J. Šponer, J. Leszczynski, P. Hobza *Structures and Energies of Hydrogen-Bonded DNA Base Pairs. A Nonempirical Study with Inclusion of Electron Correlation* *J. Phys. Chem.*, **1996**, *100*, 1965–1974.
- [20] R. Parthasarathi, R. Amutha, V. Subramanian, B. U. Nair, T. Ramasami *Bader's and Reactivity Descriptors' Analysis of DNA Base Pairs* *J. Phys. Chem. A*, **2004**, *108*, 3817–3828.

- [21] Y. Pommier, E. Leo, H. Zhang, C. Marchand *DNA Topoisomerases and Their Poisoning by Anticancer and Antibacterial Drugs* Chem. Biol., **2010**, *17*, 421–433.
- [22] R. M. Brosh Jr. *DNA helicases involved in DNA repair and their roles in cancer* Nat. Rev. Cancer, **2013**, *13*, 542–558.
- [23] T. Natsume, Y. Ishikawa, K. ichi Dedachi, N. Kurita *Density-functional calculations on DNA-DNA, PNA-DNA and PNA-PNA double strands* Chem. Phys. Lett., **2006**, *418*, 239–244.
- [24] G. Lv, F. Wei, H. Jiang, Y. Zhou, X. Wang *DFT study on the intermolecular interactions between Au_n (n=2-4) and thymine* J. Mol. Struct.: THEOCHEM, **2009**, *915*, 98–104.
- [25] J. Valdespino-Saenz, A. Martínez *Adenine-Au and adenine-uracil-Au. Non-conventional hydrogen bonds of the anions and donator-acceptor properties of the neutrals* J. Mol. Struct.: THEOCHEM, **2010**, *939*, 34–43.
- [26] Y. Maeda, A. Okamoto, Y. Hoshiba, T. Tsukamoto, Y. Ishikawa, N. Kurita *Effect of hydration on electrical conductivity of DNA duplex: Green's function study combined with DFT* Comput. Mater. Sci., **2012**, *53*, 314–320.
- [27] X. Lu, H. Shi, J. Chen, D. Ji *Theoretical study of different substituent benzenes and benzene dimers blue-shifted hydrogen bonds* Comput. Theor. Chem., **2012**, *982*, 34–39.
- [28] R. F. W. Bader; Clarendon Press: England, 1994.
- [29] N. Metropolis, A. W. Rosenbluth, M. N. Rosenbluth, A. H. Teller, E. Teller *Equation of State Calculations by Fast Computing Machines* J. Chem. Phys., **1953**, *21*, 1087–1092.
- [30] B. J. Alder, T. E. Wainwright *Phase Transition for a Hard Sphere System* J. Chem. Phys., **1957**, *27*, 1208–1209.
- [31] B. J. Alder, T. E. Wainwright *Studies in Molecular Dynamics. I. General Method* J. Chem. Phys., **1959**, *31*, 459–466.

- [32] P. Hohenberg, W. Kohn *Inhomogeneous Electron Gas* Phys. Rev., **1964**, *136*, B864–B871.
- [33] W. Kohn, L. J. Sham *Self-Consistent Equations Including Exchange and Correlation Effects* Phys. Rev., **1965**, *140*, A1133–A1138.
- [34] J. F. Janak *Proof that $\frac{\partial E}{\partial n_i} = \epsilon$ in density-functional theory* Phys. Rev. B, **1978**, *18*, 7165–7168.
- [35] A. D. Becke *A new mixing of Hartree–Fock and local density-functional theories* J. Chem. Phys., **1993**, *98*, 1372–1377.
- [36] A. D. Becke *Density-functional thermochemistry. III. The role of exact exchange* J. Chem. Phys., **1993**, *98*, 5648–5652.
- [37] A. D. Becke *Density-functional exchange-energy approximation with correct asymptotic behavior* Phys. Rev. A, **1988**, *38*, 3098–3100.
- [38] C. Lee, W. Yang, R. G. Parr *Development of the Colle-Salvetti correlation-energy formula into a functional of the electron density* Phys. Rev. B, **1988**, *37*, 785–789.
- [39] Amber 9. D. A. Case, T. A. Darden, Cheatham, C. L. Simmerling, J. Wang, R. E. Duke, R. Luo, K. M. Merz, D. A. Pearlman, M. Crowley, R. C. Walker, W. Zhang, B. Wang, S. Hayik, A. Roitberg, G. Seabra, K. F. Wong, F. Paesani, X. Wu, S. Brozell, V. Tsui, H. Gohlke, L. Yang, C. Tan, J. Mongan, V. Hornak, G. Cui, P. Beroza, D. H. Mathews, C. Schafmeister, W. S. Ross, P. A. Kollman.
- [40] T. Tsukamoto, Y. Ishikawa, Y. Sengoku, N. Kurita *A combined DFT/Green’s function study on electrical conductivity through DNA duplex between Au electrodes* Chem. Phys. Lett., **2009**, *474*, 362–365.
- [41] J. Poater, M. Swart, C. F. Guerra, F. M. Bickelhaupt *Solvent effects on hydrogen bonds in Watson-Crick, mismatched, and modified DNA base pairs* Comput. Theor. Chem., **2012**, *998*, 57–63.
- [42] W. L. Jorgensen, J. Chandrasekhar, J. D. Madura, R. W. Impey, M. L. Klein *Comparison of simple potential functions for simulating liquid water* J. Chem. Phys., **1983**, *79*, 926–935.

- [43] P. J. Hay, W. R. Wadt *Ab initio effective core potentials for molecular calculations. Potentials for the transition metal atoms Sc to Hg* J. Chem. Phys., **1985**, 82, 270–283.
- [44] W. R. Wadt, P. J. Hay *Ab initio effective core potentials for molecular calculations. Potentials for main group elements Na to Bi* J. Chem. Phys., **1985**, 82, 284–298.
- [45] P. J. Hay, W. R. Wadt *Ab initio effective core potentials for molecular calculations. Potentials for K to Au including the outermost core orbitals* J. Chem. Phys., **1985**, 82, 299–310.
- [46] A. D. Becke *Density-functional exchange-energy approximation with correct asymptotic behavior* Phys. Rev. A, **1988**, 38, 3098–3100.
- [47] B. Michlich, A. Savin, H. Stoll, H. Preuss *Results obtained with the correlation energy density functionals of becke and Lee, Yang and Parr* Chem. Phys. Lett., **1989**, 157, 200–206.
- [48] C. Lee, W. Yang, R. G. Parr *Development of the Colle-Salvetti correlation-energy formula into a functional of the electron density* Phys. Rev. B, **1988**, 37, 785–789.
- [49] Gaussian 03, Revision D.02. M. J. Frisch, G. W. Trucks, H. B. Schlegel, G. E. Scuseria, M. A. Robb, J. R. Cheeseman, J. A. Montgomery, T. Vreven, K. N. Kudin, J. C. Burant, J. M. Millam, S. S. Iyengar, J. Tomasi, V. Barone, B. Mennucci, M. Cossi, G. Scalmani, N. Rega, G. A. Petersson, H. Nakatsuji, M. Hada, M. Ehara, K. Toyota, R. Fukuda, J. Hasegawa, M. Ishida, T. Nakajima, Y. Honda, O. Kitao, H. Nakai, M. Klene, X. Li, J. E. Knox, H. P. Hratchian, J. B. Cross, V. Bakken, C. Adamo, J. Jaramillo, R. Gomperts, R. E. Stratmann, O. Yazyev, A. J. Austin, R. Cammi, C. Pomelli, J. W. Ochterski, P. Y. Ayala, K. Morokuma, G. A. Voth, P. Salvador, J. J. Dannenberg, V. G. Zakrzewski, S. Dapprich, A. D. Daniels, M. C. Strain, O. Farkas, D. K. Malick, A. D. Rabuck, K. Raghavachari, J. B. Foresman, J. V. Ortiz, Q. Cui, A. G. Baboul, S. Clifford, J. Cioslowski, B. B. Stefanov, G. Liu, A. Liashenko, P. Piskorz, I. Komaromi, R. L. Martin, D. J. Fox, T. Keith, A. M. A. Laham,

- C. Y. Peng, A. Nanayakkara, M. Challacombe, P. M. W. Gill, B. Johnson, W. Chen, M. W. Wong, C. Gonzalez, J. A. Pople.
- [50] W. Kohn, A. D. Becke, R. G. Parr *Density Functional Theory of Electronic Structure* J. Phys. Chem., **1996**, *100*, 12974–12980.
- [51] P. Hohenberg, W. Kohn *Inhomogeneous Electron Gas* Phys. Rev., **1964**, *136*, B864–B871.
- [52] W. Kohn, L. J. Sham *Self-Consistent Equations Including Exchange and Correlation Effects* Phys. Rev., **1965**, *140*, A1133–A1138.
- [53] Y. Lin, H. Wang, S. Gao, H. F. Schaefer III *Hydrogen-Bonded Proton Transfer in the Protonated Guanine-Cytosine (GC+H)⁺ Base Pair* J. Phys. Chem. B, **2011**, *115*, 11746–11756.
- [54] Y. Lin, H. Wang, S. Gao, R. Li, H. F. Schaefer III *Hydrogen-Bonded Double-Proton Transfer in Five Guanine–Cytosine Base Pairs after Hydrogen Atom Addition* J. Phys. Chem. B, **2012**, *116*, 8908–8915.
- [55] J. D. Zhang, H. F. Schaefer III *Molecular Structures and Energetics Associated with Hydrogen Atom Addition to the Guanine–Cytosine Base Pair* J. Chem. Theory Comput., **2007**, *3*, 115–126.
- [56] AIM 2000, Version 1. F. Biegler-Konig, J. Schonbohm, R. Derdau, D. Bayles, R. W. F. Bader.
- [57] U. Koch, P. L. A. Popelier *Characterization of C-H-O Hydrogen Bonds on the Basis of the Charge Density* J. Phys. Chem., **1995**, *99*, 9747–9754.
- [58] M. T. Carroll, R. F. W. Bader *An analysis of the hydrogen bond in BASE-HF complexes using the theory of atoms in molecules* Mol. Phys., **1988**, *65*, 695–722.
- [59] M. T. Carroll, C. Chang, R. F. W. Bader *Prediction of the structures of hydrogen-bonded complexes using the laplacian of the charge density* Mol. Phys., **1988**, *63*, 387–405.

- [60] B. Pullman, A. Pullman *Electron-donor and -acceptor properties of biologically important purines, pyrimidines, pteridines, flavins, and aromatic amino acids* Proc. Natl. Acad. Sci. U.S.A., **1958**, *44*, 1197–1202.
- [61] H. Berthod, C. Giessner-Prettre, A. Pullman *Theoretical study of the electronic properties of the purine and pyrimidine components of the nucleic acids* Theor. Chim. Acta, **1966**, *5*, 53–68.
- [62] B. Pullman, A. Pullman *The electronic structure of the purine-pyrimidine pairs of DNA* Biochim. Biophys. Acta, **1959**, *36*, 343 – 350.
- [63] Xu, Zhang, Li, Tao *Direct Conductance Measurement of Single DNA Molecules in Aqueous Solution* Nano Lett., **2004**, *4*, 1105–1108.
- [64] D. Porath, A. Bezryadin, S. de Vries, C. Dekker *Direct measurement of electrical transport through DNA molecules* Nature, **2000**, *403*, 635–638.
- [65] M. Xu, R. Endres, S. Tsukamoto, M. Kitamura, S. Ishida, Y. Arakawa *Conformation and Local Environment Dependent Conductance of DNA Molecules* Small, **2005**, *1*, 1168–1172.
- [66] H.-W. Fink, C. Schonberger *Electrical conduction through DNA molecules* Nature, **1999**, *398*, 407–410.
- [67] J. Bonnet, P. Yin, M. E. Ortiz, P. Subsoontorn, D. Endy *Amplifying Genetic Logic Gates* Science, **2013**, *340*, 599–603.

APPENDIX

Table A1: Topological properties of the electron density at the $(3, -1)$ bond critical point (BCP) of the hydrogen bond interactions between adenine (A) and thymine (T) base pairs

BCP	structures		ρ	$\nabla^2\rho$	λ_1	λ_2	λ_3	$ \lambda_1 /\lambda_3$	ε	$\%\Delta\varepsilon^*$	
HB1	DNA	A5'T3'	0.0252	0.0897	-0.0301	-0.0260	0.1457	0.2064	0.1585	—	
		Au-A5'T3'	0.0252	0.0877	-0.0351	-0.0331	0.1559	0.2251	0.0601	-62.11	
		A5'T3'-Au	0.0252	0.0882	-0.0350	-0.0332	0.1564	0.2237	0.0544	-65.71	
		A3'T5'	0.0643	0.0561	-0.0435	-0.0389	0.1386	0.3141	0.1174	—	
		Au-A3'T5'	0.0202	0.0743	-0.0260	-0.0247	0.1249	0.2081	0.0540	-54.05	
		A3'T5'-Au	0.0201	0.0748	-0.0259	-0.0246	0.1253	0.2068	0.0529	-54.98	
	PNA	AT	0.0978	0.0354	-0.0907	-0.0685	0.1945	0.4662	0.3238	—	
		Au-AT	0.0365	0.1255	-0.0585	-0.0560	0.2400	0.2438	0.0448	-86.18	
		AT-Au	0.0366	0.1251	-0.0586	-0.0561	0.2398	0.2444	0.0444	-86.29	
	HB2	DNA	A5'T3'	0.0433	0.0953	-0.0484	-0.0465	0.1902	0.2542	0.0396	—
			Au-A5'T3'	0.0397	0.0998	-0.0630	-0.0591	0.2218	0.2841	0.0672	69.60
			A5'T3'-Au	0.0399	0.0983	-0.0634	-0.0594	0.2210	0.2868	0.0676	70.68
PNA		AT	0.0541	0.0443	-0.0202	-0.0092	0.0737	0.2738	1.1956	—	
		Au-A3'T5'	0.0247	0.0730	-0.0334	-0.0312	0.1376	0.2431	0.0730	-93.90	
		A3'T5'-Au	0.0250	0.0719	-0.0338	-0.0315	0.1372	0.2462	0.0714	-94.03	

Continued on next page...

Table A1 – continued from previous page

BCP	structures	ρ	$\nabla^2\rho$	λ_1	λ_2	λ_3	$ \lambda_1 /\lambda_3$	ε	$\% \Delta\varepsilon^*$
PNA	AT	0.0907	0.0708	-0.0408	-0.0170	0.1286	0.3173	1.3971	—
	Au-AT	0.0389	0.0987	-0.0613	-0.0573	0.2172	0.2822	0.0706	-94.95
	AT-Au	0.0389	0.0987	-0.0613	-0.0571	0.2171	0.2824	0.0737	-94.72

* $\% \Delta\varepsilon$ is the change of the ellipticity when Au(111) stacks on adenine and thymine bases

Table A2: Topological properties of the electron density at the (3, -1) bond critical point (BCP) of the hydrogen bond interactions between guanine (G) and cytosine (C) base pairs

BCP	structures	ρ	$\nabla^2\rho$	λ_1	λ_2	λ_3	$ \lambda_1 /\lambda_3$	ε	$\%\Delta\varepsilon^*$		
HB1	DNA	G5'C3'	0.0243	0.0820	-0.0220	-0.0213	0.1253	0.1759	0.0360	—	
		Au-G5'C3'	0.0366	0.1294	-0.0589	-0.0560	0.2443	0.2412	0.0528	46.53	
		G5'C3'-Au	0.0366	0.1300	-0.0589	-0.0558	0.2448	0.2405	0.0542	50.37	
			G3'C5'	0.0272	0.0923	-0.0347	-0.0317	0.1587	0.2187	0.0963	—
			Au-G3'C5'	0.0251	0.0965	-0.0345	-0.0330	0.1640	0.2103	0.0451	-53.15
			G3'C5'-Au	0.0250	0.0973	-0.0344	-0.0330	0.1647	0.2091	0.0452	-53.02
		PNA	GC	0.0322	0.0990	-0.0424	-0.0364	0.1778	0.2382	0.1645	—
			Au-GC	0.0306	0.1097	-0.0454	-0.0432	0.1984	0.2291	0.0514	-68.77
			GC-Au	0.0308	0.1092	-0.0456	-0.0434	0.1983	0.2301	0.0508	-69.11
HB2	DNA	G5'C3'	0.0370	0.0663	-0.0141	-0.0122	0.0926	0.1522	0.1551	—	
		Au-G5'C3'	0.0323	0.0918	-0.0471	-0.0431	0.1820	0.2591	0.0946	-39.01	
		G5'C3'-Au	0.0323	0.0931	-0.0471	-0.0421	0.1823	0.2582	0.1180	-23.92	
			G3'C5'	0.0262	0.0796	-0.0279	-0.0238	0.1313	0.2127	0.1734	—
			Au-G3'C5'	0.0289	0.0833	-0.0410	-0.0381	0.1625	0.2524	0.0760	-56.19
			G3'C5'-Au	0.0287	0.0845	-0.0408	-0.0379	0.1631	0.2498	0.0751	-56.67

Continued on next page...

Table A2 – continued from previous page

BCP	structures	ρ	$\nabla^2\rho$	λ_1	λ_2	λ_3	$ \lambda_1 /\lambda_3$	ε	$\% \Delta\varepsilon^*$	
PNA	GC	0.0285	0.0625	-0.0197	-0.0179	0.1001	0.1965	0.0958	—	
	Au-GC	0.0189	0.0590	-0.0231	-0.0217	0.1037	0.2224	0.0646	-32.58	
	GC-Au	0.0190	0.0589	-0.0232	-0.0218	0.1039	0.2231	0.0622	-35.02	
HB3	DNA	G5'C3'	0.0519	0.0785	-0.0464	-0.0443	0.1692	0.2744	0.0486	—
		Au-G5'C3'	0.0435	0.1418	-0.0734	-0.0706	0.2858	0.2567	0.0394	-18.94
		G5'C3'-Au	0.0437	0.1408	-0.0736	-0.0707	0.2851	0.2581	0.0402	-17.19
	PNA	G3'C5'	0.0329	0.0739	-0.0380	-0.0349	0.1468	0.2588	0.0895	—
		Au-G3'C5'	0.0233	0.0857	-0.0310	-0.0291	0.1459	0.2127	0.0667	-25.46
		G3'C5'-Au	0.0235	0.0852	-0.0311	-0.0293	0.1456	0.2139	0.0629	-29.79
		GC	0.0183	0.0499	-0.0156	-0.0093	0.0748	0.2081	0.6726	—
Au-GC	0.0139	0.0443	-0.0157	-0.0150	0.0751	0.2095	0.0466	-93.07		
GC-Au	0.0139	0.0445	-0.0157	-0.0151	0.0754	0.2089	0.0407	-93.94		

* $\% \Delta\varepsilon$ is the change of the ellipticity when Au(111) stacks on guanine and cytosine bases

Table A3: Topological properties of the electron density at the $(3, -1)$ bond critical point (BCP) of the hydrogen bond interactions between adenine (A) and thymine (T) base pairs

BCP	structures	point charges [†]	ρ	$\nabla^2\rho$	λ_1	λ_2	λ_3	$ \lambda_1 /\lambda_3$	ε	$\%\Delta\varepsilon^*$	
HB1	DNA	Au-A5'T3'	-0.3	0.0248	0.0884	-0.0347	-0.0327	0.1557	0.2227	0.0610	1.50
			-0.2	0.0250	0.0882	-0.0348	-0.0328	0.1559	0.2234	0.0602	0.31
			-0.1	0.0251	0.0880	-0.0350	-0.0330	0.1559	0.2242	0.0600	-0.15
			0.0	0.0252	0.0877	-0.0351	-0.0331	0.1559	0.2251	0.0601	—
			0.1	0.0253	0.0874	-0.0352	-0.0332	0.1559	0.2260	0.0603	0.43
			0.2	0.0253	0.0873	-0.0353	-0.0333	0.1558	0.2264	0.0604	0.50
			0.3	0.0254	0.0870	-0.0353	-0.0333	0.1556	0.2269	0.0606	0.86
	A5'T3'-Au	-0.3	0.0252	0.0874	-0.0351	-0.0332	0.1556	0.2252	0.0564	3.80	
		-0.2	0.0252	0.0877	-0.0351	-0.0332	0.1559	0.2248	0.0556	2.28	
		-0.1	0.0252	0.0879	-0.0350	-0.0332	0.1562	0.2243	0.0549	1.02	
		0.0	0.0252	0.0882	-0.0350	-0.0332	0.1564	0.2237	0.0544	—	
		0.1	0.0251	0.0885	-0.0349	-0.0332	0.1566	0.2230	0.0538	-1.08	
		0.2	0.0251	0.0886	-0.0349	-0.0331	0.1567	0.2227	0.0528	-2.88	
		0.3	0.0250	0.0888	-0.0348	-0.0331	0.1567	0.2222	0.0517	-4.94	

Continued on next page...

Table A3 – continued from previous page

BCP	structures	point charges [†]	ρ	$\nabla^2\rho$	λ_1	λ_2	λ_3	$ \lambda_1 /\lambda_3$	ϵ	$\%\Delta\epsilon^*$
	Au-A3'T5'	-0.3	0.0201	0.0749	-0.0258	-0.0246	0.1253	0.2063	0.0520	-3.56
		-0.2	0.0201	0.0747	-0.0259	-0.0246	0.1252	0.2068	0.0525	-2.66
		-0.1	0.0201	0.0745	-0.0259	-0.0246	0.1251	0.2074	0.0532	-1.42
		0.0	0.0202	0.0743	-0.0260	-0.0247	0.1249	0.2081	0.0540	—
		0.1	0.0202	0.0740	-0.0260	-0.0247	0.1247	0.2088	0.0547	1.40
		0.2	0.0201	0.0738	-0.0260	-0.0247	0.1245	0.2092	0.0549	1.76
		0.3	0.0201	0.0735	-0.0261	-0.0247	0.1242	0.2097	0.0549	1.74
	A3'T5'-Au	-0.3	—	—	—	—	—	—	—	—
		-0.2	0.0203	0.0742	-0.0260	-0.0248	0.1249	0.2084	0.0516	-2.34
		-0.1	0.0202	0.0745	-0.0260	-0.0247	0.1251	0.2076	0.0522	-1.29
		0.0	0.0201	0.0748	-0.0259	-0.0246	0.1253	0.2068	0.0529	—
		0.1	0.0201	0.0751	-0.0258	-0.0245	0.1255	0.2060	0.0535	1.14
		0.2	0.0200	0.0752	-0.0258	-0.0245	0.1254	0.2055	0.0534	1.05
		0.3	0.0199	0.0752	-0.0257	-0.0244	0.1253	0.2052	0.0530	0.22

Continued on next page...

Table A3 – continued from previous page

BCP	structures	point charges [†]	ρ	$\nabla^2\rho$	λ_1	λ_2	λ_3	$ \lambda_1 /\lambda_3$	ϵ	$\%\Delta\epsilon^*$
PNA	Au-AT	-0.3	0.0361	0.1266	-0.0581	-0.0556	0.2403	0.2416	0.0441	-1.36
		-0.2	0.0362	0.1265	-0.0582	-0.0557	0.2403	0.2420	0.0442	-1.33
		-0.1	0.0364	0.1260	-0.0583	-0.0558	0.2402	0.2428	0.0444	-0.73
		0.0	0.0365	0.1255	-0.0585	-0.0560	0.2400	0.2438	0.0448	—
		0.1	0.0366	0.1249	-0.0586	-0.0561	0.2396	0.2446	0.0448	0.16
		0.2	0.0366	0.1245	-0.0587	-0.0562	0.2394	0.2452	0.0446	-0.30
		0.3	0.0367	0.1239	-0.0588	-0.0563	0.2390	0.2460	0.0443	-0.93
	AT-Au	-0.3	0.0365	0.1247	-0.0586	-0.0561	0.2394	0.2446	0.0439	-1.16
		-0.2	0.0366	0.1248	-0.0586	-0.0561	0.2395	0.2446	0.0439	-1.00
		-0.1	0.0366	0.1249	-0.0586	-0.0561	0.2397	0.2446	0.0442	-0.50
		0.0	0.0366	0.1251	-0.0586	-0.0561	0.2398	0.2444	0.0444	—
		0.1	0.0365	0.1250	-0.0586	-0.0561	0.2398	0.2444	0.0441	-0.75
		0.2	0.0365	0.1249	-0.0586	-0.0561	0.2397	0.2445	0.0436	-1.82
		0.3	0.0365	0.1249	-0.0586	-0.0561	0.2396	0.2444	0.0429	-3.24

Continued on next page...

Table A3 – continued from previous page

BCP	structures	point charges [†]	ρ	$\nabla^2\rho$	λ_1	λ_2	λ_3	$ \lambda_1 /\lambda_3$	ε	$\% \Delta\varepsilon^*$	
HB2	DNA	Au-A5'T3'	-0.3	0.0401	0.0975	-0.0636	-0.0596	0.2208	0.2883	0.0678	0.93
			-0.2	0.0399	0.0982	-0.0635	-0.0595	0.2211	0.2870	0.0674	0.38
			-0.1	0.0398	0.0989	-0.0633	-0.0593	0.2215	0.2856	0.0672	0.10
			0.0	0.0397	0.0998	-0.0630	-0.0591	0.2218	0.2841	0.0672	—
			0.1	0.0395	0.1006	-0.0628	-0.0588	0.2221	0.2826	0.0671	-0.13
			0.2	0.0394	0.1010	-0.0626	-0.0587	0.2222	0.2816	0.0667	-0.69
			0.3	0.0392	0.1016	-0.0624	-0.0585	0.2224	0.2804	0.0663	-1.27
	A5'T3'-Au	-0.3	0.0398	0.0992	-0.0631	-0.0592	0.2215	0.2850	0.0663	-1.88	
		-0.2	0.0398	0.0989	-0.0632	-0.0593	0.2214	0.2855	0.0666	-1.42	
		-0.1	0.0399	0.0986	-0.0633	-0.0593	0.2213	0.2861	0.0670	-0.79	
		0.0	0.0399	0.0983	-0.0634	-0.0594	0.2210	0.2868	0.0676	—	
		0.1	0.0400	0.0978	-0.0635	-0.0594	0.2207	0.2875	0.0681	0.78	
		0.2	0.0399	0.0978	-0.0634	-0.0594	0.2206	0.2875	0.0682	0.99	
		0.3	0.0399	0.0976	-0.0634	-0.0593	0.2204	0.2877	0.0683	1.12	

Continued on next page...

Table A3 – continued from previous page

BCP	structures	point charges [†]	ρ	$\nabla^2\rho$	λ_1	λ_2	λ_3	$ \lambda_1 /\lambda_3$	ϵ	$\%\Delta\epsilon^*$
	Au-A3'T5'	-0.3	0.0249	0.0719	-0.0337	-0.0313	0.1369	0.2459	0.0739	1.27
		-0.2	0.0248	0.0722	-0.0336	-0.0313	0.1371	0.2451	0.0733	0.40
		-0.1	0.0248	0.0726	-0.0335	-0.0313	0.1374	0.2442	0.0730	-0.01
		0.0	0.0247	0.0730	-0.0334	-0.0312	0.1376	0.2431	0.0730	—
		0.1	0.0246	0.0735	-0.0333	-0.0311	0.1378	0.2418	0.0732	0.31
		0.2	0.0246	0.0736	-0.0332	-0.0310	0.1379	0.2412	0.0732	0.28
		0.3	0.0245	0.0739	-0.0331	-0.0309	0.1379	0.2402	0.0730	0.10
	A3'T5'-Au	-0.3	—	—	—	—	—	—	—	—
		-0.2	0.0248	0.0728	-0.0335	-0.0313	0.1376	0.2435	0.0718	0.63
		-0.1	0.0249	0.0724	-0.0336	-0.0314	0.1374	0.2448	0.0715	0.18
		0.0	0.0250	0.0719	-0.0338	-0.0315	0.1372	0.2462	0.0714	—
		0.1	0.0251	0.0713	-0.0339	-0.0317	0.1369	0.2477	0.0713	-0.02
		0.2	0.0251	0.0710	-0.0340	-0.0317	0.1367	0.2484	0.0710	-0.44
		0.3	0.0251	0.0708	-0.0339	-0.0317	0.1365	0.2487	0.0704	-1.32

Continued on next page...

Table A3 – continued from previous page

BCP	structures	point charges [†]	ρ	$\nabla^2\rho$	λ_1	λ_2	λ_3	$ \lambda_1 /\lambda_3$	ϵ	$\%\Delta\epsilon^*$
PNA	Au-AT	-0.3	0.0393	0.0964	-0.0619	-0.0578	0.2162	0.2865	0.0708	0.22
		-0.2	0.0392	0.0969	-0.0618	-0.0577	0.2164	0.2856	0.0705	-0.08
		-0.1	0.0390	0.0977	-0.0616	-0.0575	0.2168	0.2840	0.0705	-0.10
		0.0	0.0389	0.0987	-0.0613	-0.0573	0.2172	0.2822	0.0706	—
		0.1	0.0387	0.0995	-0.0610	-0.0570	0.2176	0.2805	0.0705	-0.14
		0.2	0.0385	0.1002	-0.0608	-0.0568	0.2178	0.2792	0.0703	-0.49
		0.3	0.0383	0.1009	-0.0605	-0.0566	0.2180	0.2777	0.0699	-1.02
	AT-Au	-0.3	0.0386	0.0998	-0.0609	-0.0567	0.2173	0.2802	0.0748	1.47
		-0.2	0.0387	0.0995	-0.0610	-0.0568	0.2173	0.2809	0.0742	0.74
		-0.1	0.0388	0.0991	-0.0612	-0.0570	0.2173	0.2816	0.0739	0.27
		0.0	0.0389	0.0987	-0.0613	-0.0571	0.2171	0.2824	0.0737	—
		0.1	0.0389	0.0985	-0.0614	-0.0572	0.2171	0.2828	0.0734	-0.35
		0.2	0.0390	0.0983	-0.0614	-0.0572	0.2170	0.2830	0.0731	-0.75
		0.3	0.0390	0.0981	-0.0615	-0.0573	0.2168	0.2834	0.0728	-1.23

* $\%\Delta\epsilon$ is the change of the ellipticity when Au(111) stacks on adenine and thymine bases.

[†]A positive value is the applying of the electric field by stacking positive charges above the Au(111) surface and negative charges under the base. A negative value is the reverse of the electric field direction, conforming to a positive value.

Table A4: Topological properties of the electron density at the $(3, -1)$ bond critical point (BCP) of the hydrogen bond interactions between guanine (G) and cytosine (C) base pairs

BCP	structures		point charges [†]	ρ	$\nabla^2\rho$	λ_1	λ_2	λ_3	$ \lambda_1 /\lambda_3$	ε	$\%\Delta\varepsilon^*$
HB1	DNA	Au-G5'C3'	-0.3	0.0366	0.1308	-0.0587	-0.0557	0.2452	0.2394	0.0547	3.49
			-0.2	0.0366	0.1305	-0.0588	-0.0557	0.2450	0.2398	0.0542	2.72
			-0.1	0.0366	0.1300	-0.0588	-0.0558	0.2447	0.2404	0.0536	1.43
			0.0	0.0366	0.1294	-0.0589	-0.0560	0.2443	0.2412	0.0528	—
			0.1	0.0366	0.1288	-0.0590	-0.0561	0.2438	0.2419	0.0519	-1.75
			0.2	0.0366	0.1283	-0.0590	-0.0561	0.2434	0.2423	0.0509	-3.59
			0.3	0.0365	0.1277	-0.0590	-0.0562	0.2429	0.2430	0.0498	-5.79
	G5'C3'-Au	-0.3	0.0364	0.1307	-0.0586	-0.0555	0.2448	0.2393	0.0550	1.44	
		-0.2	0.0365	0.1305	-0.0587	-0.0556	0.2448	0.2398	0.0547	0.91	
		-0.1	0.0365	0.1303	-0.0588	-0.0558	0.2448	0.2402	0.0545	0.48	
		0.0	0.0366	0.1300	-0.0589	-0.0558	0.2448	0.2405	0.0542	—	
		0.1	0.0366	0.1296	-0.0590	-0.0560	0.2445	0.2411	0.0536	-1.18	
		0.2	0.0366	0.1292	-0.0590	-0.0561	0.2442	0.2416	0.0527	-2.78	
		0.3	0.0366	0.1286	-0.0591	-0.0562	0.2438	0.2422	0.0514	-5.16	

Continued on next page...

Table A4 – continued from previous page

BCP	structures	point charges [†]	ρ	$\nabla^2\rho$	λ_1	λ_2	λ_3	$ \lambda_1 /\lambda_3$	ϵ	$\%\Delta\epsilon^*$
	Au-G3'C5'	-0.3	0.0249	0.0970	-0.0343	-0.0328	0.1641	0.2088	0.0433	-3.92
		-0.2	0.0250	0.0969	-0.0343	-0.0329	0.1641	0.2092	0.0438	-2.84
		-0.1	0.0250	0.0967	-0.0344	-0.0330	0.1641	0.2097	0.0444	-1.50
		0.0	0.0251	0.0965	-0.0345	-0.0330	0.1640	0.2103	0.0451	—
		0.1	0.0252	0.0962	-0.0346	-0.0330	0.1638	0.2109	0.0457	1.34
		0.2	0.0252	0.0960	-0.0346	-0.0330	0.1637	0.2112	0.0461	2.11
		0.3	0.0252	0.0957	-0.0346	-0.0331	0.1633	0.2118	0.0459	1.83
	G3'C5'-Au	-0.3	—	—	—	—	—	—	—	—
		-0.2	0.0252	0.0963	-0.0346	-0.0331	0.1640	0.2109	0.0446	-1.35
		-0.1	0.0251	0.0968	-0.0345	-0.0330	0.1644	0.2101	0.0449	-0.69
		0.0	0.0250	0.0973	-0.0344	-0.0330	0.1647	0.2091	0.0452	—
		0.1	0.0250	0.0975	-0.0344	-0.0329	0.1648	0.2086	0.0451	-0.27
		0.2	0.0249	0.0974	-0.0343	-0.0329	0.1647	0.2086	0.0440	-2.64
		0.3	0.0249	0.0968	-0.0343	-0.0330	0.1641	0.2093	0.0418	-7.56

Continued on next page...

Table A4 – continued from previous page

BCP	structures	point charges [†]	ρ	$\nabla^2\rho$	λ_1	λ_2	λ_3	$ \lambda_1 /\lambda_3$	ϵ	$\% \Delta\epsilon^*$
PNA	Au-GC	-0.3	0.0307	0.1095	-0.0455	-0.0433	0.1982	0.2295	0.0516	0.37
		-0.2	0.0306	0.1101	-0.0454	-0.0432	0.1986	0.2285	0.0516	0.44
		-0.1	0.0306	0.1100	-0.0454	-0.0432	0.1986	0.2286	0.0515	0.29
		0.0	0.0306	0.1097	-0.0454	-0.0432	0.1984	0.2291	0.0514	—
		0.1	0.0306	0.1095	-0.0455	-0.0433	0.1982	0.2295	0.0513	-0.21
		0.2	0.0306	0.1092	-0.0455	-0.0433	0.1980	0.2298	0.0511	-0.59
		0.3	0.0306	0.1086	-0.0455	-0.0434	0.1975	0.2307	0.0505	-1.71
	GC-Au	-0.3	0.0307	0.1081	-0.0456	-0.0435	0.1972	0.2314	0.0492	-3.23
		-0.2	0.0307	0.1085	-0.0456	-0.0435	0.1976	0.2310	0.0496	-2.39
		-0.1	0.0307	0.1089	-0.0456	-0.0435	0.1980	0.2305	0.0502	-1.25
		0.0	0.0308	0.1092	-0.0456	-0.0434	0.1983	0.2301	0.0508	—
		0.1	0.0308	0.1094	-0.0456	-0.0434	0.1984	0.2300	0.0515	1.26
		0.2	0.0308	0.1094	-0.0456	-0.0434	0.1985	0.2300	0.0519	2.13
		0.3	0.0308	0.1090	-0.0457	-0.0435	0.1982	0.2305	0.0515	1.27

Continued on next page...

Table A4 – continued from previous page

BCP	structures		point charges [†]	ρ	$\nabla^2\rho$	λ_1	λ_2	λ_3	$ \lambda_1 /\lambda_3$	ϵ	$\% \Delta\epsilon^*$
HB2	DNA	Au-G5'C3'	-0.3	0.0320	0.0930	-0.0467	-0.0426	0.1822	0.2561	0.0968	2.35
			-0.2	0.0320	0.0927	-0.0468	-0.0427	0.1822	0.2568	0.0960	1.46
			-0.1	0.0322	0.0923	-0.0470	-0.0429	0.1821	0.2579	0.0952	0.61
			0.0	0.0323	0.0918	-0.0471	-0.0431	0.1820	0.2591	0.0946	—
			0.1	0.0324	0.0912	-0.0473	-0.0432	0.1817	0.2602	0.0940	-0.60
			0.2	0.0325	0.0909	-0.0474	-0.0433	0.1816	0.2609	0.0934	-1.28
			0.3	0.0326	0.0904	-0.0475	-0.0434	0.1813	0.2619	0.0929	-1.83
	G5'C3'-Au	-0.3	0.0318	0.0938	-0.0464	-0.0414	0.1816	0.2556	0.1212	2.75	
		-0.2	0.0320	0.0935	-0.0467	-0.0417	0.1819	0.2565	0.1194	1.16	
		-0.1	0.0321	0.0933	-0.0469	-0.0419	0.1821	0.2574	0.1183	0.26	
		0.0	0.0323	0.0931	-0.0471	-0.0421	0.1823	0.2582	0.1180	—	
		0.1	0.0324	0.0928	-0.0472	-0.0423	0.1823	0.2592	0.1180	0.03	
		0.2	0.0325	0.0924	-0.0474	-0.0424	0.1822	0.2601	0.1185	0.43	
		0.3	0.0326	0.0921	-0.0475	-0.0425	0.1821	0.2611	0.1196	1.33	

Continued on next page...

Table A4 – continued from previous page

BCP	structures	point charges [†]	ρ	$\nabla^2\rho$	λ_1	λ_2	λ_3	$ \lambda_1 /\lambda_3$	ϵ	$\% \Delta\epsilon^*$
	Au-G3'C5'	-0.3	0.0287	0.0841	-0.0408	-0.0380	0.1628	0.2506	0.0751	-1.23
		-0.2	0.0288	0.0839	-0.0409	-0.0380	0.1628	0.2511	0.0752	-1.11
		-0.1	0.0288	0.0836	-0.0409	-0.0381	0.1626	0.2517	0.0755	-0.67
		0.0	0.0289	0.0833	-0.0410	-0.0381	0.1625	0.2524	0.0760	—
		0.1	0.0289	0.0830	-0.0411	-0.0382	0.1622	0.2533	0.0766	0.78
		0.2	0.0289	0.0828	-0.0411	-0.0382	0.1620	0.2537	0.0769	1.22
		0.3	0.0289	0.0824	-0.0411	-0.0382	0.1617	0.2544	0.0772	1.60
	G3'C5'-Au	-0.3	—	—	—	—	—	—	—	—
		-0.2	0.0290	0.0831	-0.0412	-0.0383	0.1626	0.2533	0.0754	0.36
		-0.1	0.0289	0.0838	-0.0410	-0.0381	0.1629	0.2516	0.0752	0.13
		0.0	0.0287	0.0845	-0.0408	-0.0379	0.1631	0.2498	0.0751	—
		0.1	0.0286	0.0848	-0.0406	-0.0378	0.1632	0.2488	0.0749	-0.31
		0.2	0.0285	0.0849	-0.0405	-0.0377	0.1631	0.2484	0.0746	-0.76
		0.3	0.0284	0.0843	-0.0405	-0.0377	0.1626	0.2492	0.0740	-1.51

Continued on next page...

Table A4 – continued from previous page

BCP	structures	point charges [†]	ρ	$\nabla^2\rho$	λ_1	λ_2	λ_3	$ \lambda_1 /\lambda_3$	ϵ	$\% \Delta\epsilon^*$
PNA	Au-GC	-0.3	0.0189	0.0590	-0.0230	-0.0216	0.1035	0.2223	0.0674	4.37
		-0.2	0.0188	0.0591	-0.0230	-0.0215	0.1036	0.2215	0.0662	2.53
		-0.1	0.0188	0.0591	-0.0230	-0.0216	0.1037	0.2218	0.0652	0.93
		0.0	0.0189	0.0590	-0.0231	-0.0217	0.1037	0.2224	0.0646	—
		0.1	0.0189	0.0589	-0.0231	-0.0217	0.1037	0.2228	0.0643	-0.43
		0.2	0.0190	0.0587	-0.0231	-0.0217	0.1036	0.2232	0.0640	-0.96
		0.3	0.0190	0.0585	-0.0232	-0.0218	0.1034	0.2240	0.0636	-1.57
	GC-Au	-0.3	0.0191	0.0583	-0.0233	-0.0219	0.1035	0.2247	0.0616	-1.06
		-0.2	0.0191	0.0585	-0.0232	-0.0219	0.1036	0.2242	0.0614	-1.32
		-0.1	0.0191	0.0587	-0.0232	-0.0219	0.1038	0.2236	0.0617	-0.84
		0.0	0.0190	0.0589	-0.0232	-0.0218	0.1039	0.2231	0.0622	—
		0.1	0.0190	0.0589	-0.0232	-0.0218	0.1039	0.2230	0.0627	0.72
		0.2	0.0190	0.0589	-0.0231	-0.0218	0.1038	0.2229	0.0632	1.60
		0.3	0.0190	0.0588	-0.0231	-0.0218	0.1037	0.2232	0.0636	2.11

Continued on next page...

Table A4 – continued from previous page

BCP	structures	point charges [†]	ρ	$\nabla^2\rho$	λ_1	λ_2	λ_3	$ \lambda_1 /\lambda_3$	ϵ	$\%\Delta\epsilon^*$	
HB3	DNA	Au-G5'C3'	-0.3	0.0437	0.1406	-0.0735	-0.0707	0.2848	0.2582	0.0406	3.07
			-0.2	0.0437	0.1408	-0.0735	-0.0707	0.2850	0.2579	0.0399	1.39
			-0.1	0.0436	0.1413	-0.0734	-0.0706	0.2853	0.2574	0.0397	0.75
			0.0	0.0435	0.1418	-0.0734	-0.0706	0.2858	0.2567	0.0394	—
			0.1	0.0434	0.1424	-0.0732	-0.0705	0.2861	0.2560	0.0388	-1.53
			0.2	0.0433	0.1427	-0.0731	-0.0705	0.2863	0.2555	0.0380	-3.55
			0.3	0.0432	0.1432	-0.0730	-0.0704	0.2865	0.2547	0.0370	-6.11
	G5'C3'-Au	-0.3	0.0437	0.1406	-0.0735	-0.0706	0.2847	0.2582	0.0410	2.05	
		-0.2	0.0437	0.1407	-0.0735	-0.0707	0.2849	0.2581	0.0408	1.33	
		-0.1	0.0437	0.1408	-0.0736	-0.0707	0.2851	0.2581	0.0405	0.69	
		0.0	0.0437	0.1408	-0.0736	-0.0707	0.2851	0.2581	0.0402	—	
		0.1	0.0436	0.1412	-0.0735	-0.0707	0.2854	0.2576	0.0397	-1.40	
		0.2	0.0436	0.1415	-0.0734	-0.0707	0.2856	0.2571	0.0389	-3.17	
		0.3	0.0435	0.1418	-0.0733	-0.0706	0.2857	0.2566	0.0380	-5.61	

Continued on next page...

Table A4 – continued from previous page

BCP	structures	point charges [†]	ρ	$\nabla^2\rho$	λ_1	λ_2	λ_3	$ \lambda_1 /\lambda_3$	ϵ	$\%\Delta\epsilon^*$
Au-G3'C5'		-0.3	0.0232	0.0852	-0.0309	-0.0288	0.1448	0.2130	0.0703	5.29
		-0.2	0.0232	0.0853	-0.0309	-0.0289	0.1452	0.2130	0.0687	2.92
		-0.1	0.0233	0.0855	-0.0310	-0.0290	0.1455	0.2129	0.0675	1.15
		0.0	0.0233	0.0857	-0.0310	-0.0291	0.1459	0.2127	0.0667	—
		0.1	0.0234	0.0860	-0.0310	-0.0291	0.1462	0.2123	0.0662	-0.80
		0.2	0.0234	0.0862	-0.0310	-0.0291	0.1463	0.2120	0.0654	-2.04
		0.3	0.0233	0.0865	-0.0310	-0.0291	0.1465	0.2113	0.0641	-3.94
G3'C5'-Au		-0.3	—	—	—	—	—	—	—	—
		-0.2	0.0232	0.0861	-0.0309	-0.0290	0.1460	0.2116	0.0638	1.46
		-0.1	0.0233	0.0856	-0.0310	-0.0292	0.1458	0.2127	0.0632	0.59
		0.0	0.0235	0.0852	-0.0311	-0.0293	0.1456	0.2139	0.0629	—
		0.1	0.0235	0.0849	-0.0312	-0.0294	0.1455	0.2144	0.0622	-1.05
		0.2	0.0235	0.0849	-0.0312	-0.0294	0.1454	0.2144	0.0608	-3.26
		0.3	0.0234	0.0852	-0.0311	-0.0293	0.1456	0.2133	0.0582	-7.46

Continued on next page...

Table A4 – continued from previous page

BCP	structures	point charges [†]	ρ	$\nabla^2\rho$	λ_1	λ_2	λ_3	$ \lambda_1 /\lambda_3$	ε	$\%\Delta\varepsilon^*$
PNA	Au-GC	-0.3	0.0138	0.0444	-0.0157	-0.0149	0.0749	0.2089	0.0505	8.34
		-0.2	0.0138	0.0442	-0.0157	-0.0150	0.0749	0.2096	0.0486	4.30
		-0.1	0.0139	0.0443	-0.0157	-0.0150	0.0750	0.2097	0.0474	1.60
		0.0	0.0139	0.0443	-0.0157	-0.0150	0.0751	0.2095	0.0466	—
		0.1	0.0139	0.0444	-0.0157	-0.0150	0.0752	0.2092	0.0461	-1.02
		0.2	0.0138	0.0445	-0.0157	-0.0150	0.0752	0.2088	0.0455	-2.46
		0.3	0.0137	0.0446	-0.0156	-0.0150	0.0752	0.2079	0.0447	-4.06
	GC-Au	-0.3	0.0138	0.0449	-0.0156	-0.0150	0.0755	0.2068	0.0410	0.58
		-0.2	0.0138	0.0448	-0.0157	-0.0151	0.0755	0.2075	0.0407	-0.02
		-0.1	0.0139	0.0446	-0.0157	-0.0151	0.0754	0.2083	0.0408	0.10
		0.0	0.0139	0.0445	-0.0157	-0.0151	0.0754	0.2089	0.0407	—
		0.1	0.0139	0.0444	-0.0157	-0.0151	0.0753	0.2089	0.0402	-1.35
		0.2	0.0138	0.0444	-0.0157	-0.0151	0.0752	0.2089	0.0395	-3.12
		0.3	0.0138	0.0444	-0.0156	-0.0151	0.0751	0.2082	0.0378	-7.28

* $\%\Delta\varepsilon$ is the change of the ellipticity when Au(111) stacks on guanine and cytosine bases

[†]A positive value is the applying of the electric field by stacking positive charges above the Au(111) surface and negative charges under the base. A negative value is the reverse of the electric field direction, conforming to a positive value.

Table A5: Bond path length (a.u.) of the $(3, -1)$ bond critical point (BCP) to each nuclei associated with the hydrogen bonds between adenine (A) and thymine (T) base pairs

structures	point charges*	HB1			HB2			
		BCP-O	BCP-H	total	BCP-H	BCP-N	total	
DNA Au-A5'T3'	-0.3	2.3858	1.3458	3.7316	1.1888	2.3286	3.5174	
	-0.2	2.3862	1.3449	3.7312	1.1897	2.3277	3.5174	
	-0.1	2.3868	1.3440	3.7308	1.1907	2.3268	3.5176	
	0.0	2.3876	1.3429	3.7305	1.1920	2.3257	3.5177	
	0.1	2.3884	1.3418	3.7302	1.1932	2.3247	3.5179	
	0.2	2.3888	1.3413	3.7301	1.1939	2.3242	3.5181	
	0.3	2.3895	1.3405	3.7300	1.1949	2.3234	3.5183	
	A5'T3'-Au	-0.3	2.3887	1.3427	3.7313	1.1916	2.3260	3.5176
		-0.2	2.3877	1.3433	3.7310	1.1912	2.3265	3.5176
		-0.1	2.3866	1.3440	3.7306	1.1908	2.3270	3.5178
		0.0	2.3854	1.3449	3.7303	1.1903	2.3277	3.5179
		0.1	2.3842	1.3459	3.7300	1.1897	2.3284	3.5181
		0.2	2.3837	1.3462	3.7299	1.1897	2.3286	3.5183
		0.3	2.3830	1.3468	3.7298	1.1895	2.3290	3.5185

Continued on next page...

Table A5 – continued from previous page

structures	point charges*	HB1			HB2		
		BCP-O	BCP-H	total	BCP-H	BCP-N	total
Au-A3'T5'	-0.3	2.4504	1.4352	3.8856	1.3614	2.5355	3.8969
	-0.2	2.4517	1.4344	3.8861	1.3623	2.5343	3.8966
	-0.1	2.4532	1.4335	3.8867	1.3634	2.5329	3.8963
	0.0	2.4549	1.4324	3.8873	1.3648	2.5313	3.8961
	0.1	2.4569	1.4310	3.8879	1.3665	2.5294	3.8959
	0.2	2.4580	1.4305	3.8885	1.3673	2.5286	3.8959
	0.3	2.4598	1.4294	3.8892	1.3685	2.5274	3.8959
A3'T5'-Au	-0.3	—	—	—	—	—	—
	-0.2	2.4552	1.4312	3.8864	1.3648	2.5315	3.8963
	-0.1	2.4537	1.4331	3.8867	1.3631	2.5332	3.8963
	0.0	2.4521	1.4351	3.8872	1.3614	2.5350	3.8964
	0.1	2.4504	1.4372	3.8876	1.3596	2.5369	3.8965
	0.2	2.4498	1.4383	3.8881	1.3587	2.5379	3.8966
	0.3	2.4497	1.4390	3.8887	1.3582	2.5385	3.8967

Continued on next page...

Table A5 – continued from previous page

structures		point charges*	HB1			HB2		
			BCP-O	BCP-H	total	BCP-H	BCP-N	total
PNA	Au-AT	-0.3	2.2194	1.2033	3.4227	1.1971	2.3343	3.5314
		-0.2	2.2196	1.2028	3.4225	1.1977	2.3338	3.5315
		-0.1	2.2204	1.2019	3.4223	1.1990	2.3326	3.5316
		0.0	2.2214	1.2008	3.4222	1.2004	2.3314	3.5318
		0.1	2.2224	1.1998	3.4222	1.2018	2.3301	3.5319
		0.2	2.2231	1.1990	3.4221	1.2028	2.3292	3.5321
		0.3	2.2241	1.1980	3.4222	1.2041	2.3281	3.5322
	AT-Au	-0.3	2.2228	1.1991	3.4219	1.2025	2.3301	3.5326
		-0.2	2.2227	1.1993	3.4220	1.2020	2.3303	3.5323
		-0.1	2.2226	1.1995	3.4221	1.2015	2.3306	3.5321
		0.0	2.2224	1.1998	3.4222	1.2010	2.3309	3.5319
		0.1	2.2224	1.1999	3.4224	1.2007	2.3311	3.5318
		0.2	2.2226	1.1999	3.4225	1.2005	2.3311	3.5317
		0.3	2.2227	1.2000	3.4227	1.2002	2.3314	3.5316

*A positive value is the applying of the electric field by stacking positive charges above the Au(111) surface and negative charges under the base. A negative value is the reverse of the electric field direction, conforming to a positive value.

Table A6: Bond path length (a.u.) of the $(3, -1)$ bond critical point (BCP) to each nuclei associated with the hydrogen bonds between guanine (G) and cytosine (C) base pairs

structures		point charges*	HB1			HB2			HB3		
			BCP-O	BCP-H	total	BCP-N	BCP-H	total	BCP-H	BCP-O	total
DNA	Au-G5'C3'	-0.3	2.2060	1.1975	3.4035	2.3929	1.2943	3.6872	1.1391	2.1588	3.2979
		-0.2	2.2065	1.1970	3.4036	2.3934	1.2934	3.6868	1.1394	2.1586	3.2980
		-0.1	2.2074	1.1964	3.4038	2.3942	1.2920	3.6862	1.1400	2.1580	3.2981
		0.0	2.2084	1.1956	3.4040	2.3952	1.2904	3.6856	1.1408	2.1574	3.2982
		0.1	2.2095	1.1948	3.4043	2.3963	1.2890	3.6852	1.1416	2.1567	3.2983
		0.2	2.2102	1.1943	3.4045	2.3970	1.2880	3.6849	1.1421	2.1563	3.2984
		0.3	2.2112	1.1935	3.4048	2.3980	1.2867	3.6847	1.1428	2.1557	3.2986
	G5'C3'-Au	-0.3	2.2062	1.1973	3.4035	2.3923	1.2946	3.6869	1.1389	2.1590	3.2980
		-0.2	2.2066	1.1970	3.4036	2.3924	1.2938	3.6862	1.1392	2.1588	3.2980
		-0.1	2.2071	1.1967	3.4038	2.3925	1.2930	3.6856	1.1395	2.1587	3.2982
		0.0	2.2075	1.1964	3.4039	2.3925	1.2924	3.6849	1.1397	2.1586	3.2983
		0.1	2.2084	1.1958	3.4042	2.3931	1.2914	3.6845	1.1403	2.1581	3.2985
		0.2	2.2092	1.1952	3.4044	2.3937	1.2905	3.6842	1.1409	2.1577	3.2986
		0.3	2.2102	1.1944	3.4046	2.3943	1.2896	3.6839	1.1415	2.1573	3.2988

Continued on next page. . .

Table A6 – continued from previous page

structures	point charges*	HB1			HB2			HB3		
		BCP-O	BCP-H	total	BCP-N	BCP-H	total	BCP-H	BCP-O	total
Au-G3'C5'	-0.3	2.3428	1.3429	3.6857	2.4530	1.3131	3.7661	1.3895	2.4004	3.7899
	-0.2	2.3433	1.3424	3.6857	2.4537	1.3127	3.7663	1.3895	2.3995	3.7890
	-0.1	2.3440	1.3417	3.6858	2.4545	1.3121	3.7666	1.3897	2.3984	3.7881
	0.0	2.3450	1.3409	3.6859	2.4556	1.3114	3.7670	1.3900	2.3972	3.7872
	0.1	2.3462	1.3399	3.6861	2.4569	1.3105	3.7674	1.3907	2.3957	3.7864
	0.2	2.3468	1.3394	3.6863	2.4577	1.3101	3.7678	1.3912	2.3948	3.7859
	0.3	2.3482	1.3383	3.6866	2.4589	1.3093	3.7682	1.3923	2.3932	3.7855
G3'C5'-Au	-0.3	—	—	—	—	—	—	—	—	—
	-0.2	2.3459	1.3397	3.6856	2.4564	1.3099	3.7663	1.3928	2.3962	3.7890
	-0.1	2.3440	1.3415	3.6855	2.4545	1.3120	3.7665	1.3905	2.3977	3.7882
	0.0	2.3420	1.3434	3.6854	2.4525	1.3142	3.7667	1.3881	2.3995	3.7875
	0.1	2.3410	1.3444	3.6854	2.4515	1.3154	3.7670	1.3869	2.4002	3.7870
	0.2	2.3411	1.3445	3.6856	2.4515	1.3158	3.7673	1.3867	2.4000	3.7866
	0.3	2.3432	1.3429	3.6861	2.4532	1.3145	3.7677	1.3882	2.3980	3.7863

Continued on next page...

Table A6 – continued from previous page

structures		point charges*	HB1			HB2			HB3		
			BCP-O	BCP-H	total	BCP-N	BCP-H	total	BCP-H	BCP-O	total
PNA	Au-GC	-0.3	2.2911	1.2719	3.5630	2.6429	1.4742	4.1170	1.5677	2.6838	4.2514
		-0.2	2.2895	1.2734	3.5629	2.6408	1.4759	4.1167	1.5660	2.6855	4.2514
		-0.1	2.2897	1.2734	3.5631	2.6407	1.4758	4.1165	1.5660	2.6853	4.2513
		0.0	2.2904	1.2729	3.5633	2.6414	1.4750	4.1164	1.5667	2.6844	4.2511
		0.1	2.2911	1.2725	3.5635	2.6420	1.4744	4.1164	1.5674	2.6836	4.2510
		0.2	2.2917	1.2720	3.5638	2.6426	1.4738	4.1164	1.5681	2.6829	4.2510
		0.3	2.2933	1.2708	3.5641	2.6443	1.4723	4.1165	1.5699	2.6810	4.2510
GC-Au		-0.3	2.2947	1.2693	3.5641	2.6468	1.4699	4.1167	1.5721	2.6785	4.2507
		-0.2	2.2937	1.2701	3.5638	2.6455	1.4711	4.1165	1.5708	2.6799	4.2507
		-0.1	2.2926	1.2709	3.5635	2.6440	1.4724	4.1165	1.5695	2.6813	4.2508
		0.0	2.2919	1.2714	3.5633	2.6431	1.4734	4.1165	1.5686	2.6824	4.2509
		0.1	2.2917	1.2715	3.5632	2.6429	1.4736	4.1165	1.5685	2.6826	4.2511
		0.2	2.2916	1.2715	3.5631	2.6428	1.4738	4.1166	1.5684	2.6828	4.2512
		0.3	2.2926	1.2706	3.5632	2.6439	1.4729	4.1168	1.5696	2.6817	4.2514

*A positive value is the applying of the electric field by stacking positive charges above the Au(111) surface and negative charges under the base. A negative value is the reverse of the electric field direction, conforming to a positive value.

Table A7: Energy gap profiles of the base pair structures combined with Au(111) were applied in the electric field.

structures			point charges						†
			-0.3	-0.2	-0.1	0.0	0.1	0.2	
AT	DNA	Au-A5'T3'	0.047	0.090	0.060	0.031	0.008	0.008	0.007
		A5'T3'-Au	0.045	0.089	0.060	0.031	0.008	0.007	0.008
		Au-A3'T5'	0.038	0.085	0.074	0.042	0.008	0.009	0.009
		A3'T5'-Au	—	0.091	0.067	0.038	0.010	0.007	0.007
	PNA	Au-AT	0.009	0.022	0.023	0.020	0.001	0.011	0.011
		AT-Au	0.016	0.025	0.029	0.015	0.010	0.010	0.010
GC	DNA	Au-G5'C3'	0.012	0.083	0.056	0.018	0.008	0.007	0.007
		G5'C3'-Au	0.053	0.069	0.040	0.011	0.008	0.008	0.008
		Au-G3'C5'	0.042	0.081	0.057	0.031	0.011	0.009	0.009
		G3'C5'-Au	—	0.065	0.036	0.006	0.007	0.007	0.007
	PNA	Au-GC	0.010	0.011	0.009	0.008	0.008	0.013	0.013
		GC-Au	0.025	0.024	0.022	0.009	0.009	0.009	0.009

†A positive value is the applying of the electric field by stacking positive charges above the Au(111) surface and negative charges under the base. A negative value is the reverse of the electric field direction, conforming to a positive value.

VITAE

Personal Details

Name	Mr.Thitiphong Meenayothin
Date of Birth	February 15, 1989
Place of Birth	Bangkok, Thailand
Address	61/60 Ratchaprarop Road, Makkasan, Ratchathewi, Bangkok 10400, Thailand
Telephone	089-7674662
E-mail address	bas.tmee@gmail.com

Education

2011-2014	M.Sc. in Chemistry, Chulalongkorn University, Thailand
2007-2011	B.Sc. in Chemistry (Major: Chemistry; Minor: Entrepreneurship), Chulalongkorn University, Thailand
2004-2007	Rajavinit Mathayom School, Bangkok, Thailand
1994-2004	Maepra Fatima School, Bangkok, Thailand

Presentation

Thitiphong Meenayothin, Viwat Vchirawongkwin “Effect of Au(111) on hydrogen bonds in DNA and PNA base pairs” *The 18th International Annual Symposium on Computational Science and Engineering*, Kasetsart University, Sriracha Campus, Ambassador City Jomtien, Chonburi, Thailand, March 17-19, **2014**, pp 8-15.